IEEE Access
Multidisciplinary | Rapid Review | Open Access Journal

Received May 15, 2019, accepted June 5, 2019, date of publication June 24, 2019, date of current version July 15, 2019.

Digital Object Identifier 10.1109/ACCESS.2019.2924704

Cooperative Spectrum Sensing in Multichannel Cognitive Radio Networks With Energy Harvesting

AKINBODE A. OLAWOLE, FAMBIRAI TAKAWIRA, (Member, IEEE), AND OLUTAYO O. OYERINDE, (Senior Member, IEEE)
School of Electrical and Information Engineering, University of the Witwatersrand, Johannesburg 2050, South Africa
Corresponding author: Akinbode A. Olawole (alexolawole@gmail.com)

ABSTRACT This paper investigates cooperative spectrum sensing in multi-channel cognitive radio networks (CRNs) with energy harvesting. Our goal is two-fold: first, to determine the optimal sensing parameters for effective management of the limited energy budget in order to maximize the achievable throughput, and second, to exploit the benefits of a practical CRN towards improving the performance of the energy constrained CRN. Two different scenarios are considered. In the first, the secondary user (SU) is assigned a single radio frequency (RF) harvesting source, while in the second, the SU is assigned multiple RF harvesting sources and can opportunistically harvest from any of the sources. For these scenarios, the problem is formulated as a stochastic optimal control system with infinite and continuous state and action spaces. This is known to be computationally intractable and becomes even more complicated in a two-dimensional problem such as considered. In order to reduce the computational complexity, a myopic optimization approach is taken, and the problem is formulated into a mixed integer nonlinear problem (MINLP) to determine the channel assignment, the sensing duration, the distribution of the sensing duration associated with the assigned channels and the detection threshold under the constraint of energy causality and primary user (PU) protection. A near-optimal solution is obtained to the MINLP based on the alternating convex optimization technique. The simulation results obtained show that the considered work can improve the amount of energy harvested and, by extension, the active probability of the SUs by exploiting the multi-channel benefits of practical CRN for enhanced throughput.

INDEX TERMS Energy harvesting cognitive radio network (EH-CRN), cooperative spectrum sensing, energy harvesting sources, primary user (PU), multi-channel, optimization problem.

I. INTRODUCTION

Recent development in energy harvesting [1]–[4] has initiated research efforts towards exploiting the possibility of alternative energy supply to the A.C rechargeable/replaceable batteries in cognitive radios. This intends to jointly reduce energy cost and deal with the problem of having to replace batteries, promising a cognitive radio system with cheaper and more convenient energy supply. In the RF energy harvesting-based scheme, spectrum sensing and data transmission activities of the SU can only occur with enough harvested RF energy (a phenomenon referred to as energy causality). The system is however a stochastic process in terms of the secondary user energy state over time. The energy level at the beginning of each frame depends on the residual energy and the action taken in the previous frame. The RF energy arrival is also intermittent and random, while the magnitude of the electrical energy derived from the harvested RF may not always be sufficient to maximize throughput. It is therefore imperative that the CRN is energy efficient in terms of balancing the energy consumption during sensing and transmission activities with the amount of energy harvested. In the conventional cognitive radio networks (which can otherwise be referred to as unconstrained energy counterpart), a sensing-throughput trade-off [5] exists, which hinges on the sensing time and sensing accuracy. However, in the context of energy harvesting CRN, the outcomes of the sensing process (i.e. the sensing time and sensing accuracy)

The associate editor coordinating the review of this manuscript and approving it for publication was Antonino Orsino.

are energy constrained, making the energy harvesting-based CRN (EH-CRN) a more complicated scenario.

A. RELATED WORKS

The effect of energy arrival rate on spectrum sensing and access policy in EH-CRN is investigated in [6] and [7], where the authors formulated the problem as a constrained partially observable Markov decision process (POMDP). In particular, the studies in [6] identify the optimal sensing policy, while [7] is an extension of [6] that determines the optimal sensing policy and detection threshold that maximizes the expected total throughput under energy causality and collision constraints. Chung *et al.* [8] investigated the relationship between the optimal sensing duration and the corresponding sensing threshold with the purpose of conserving energy while the average throughput is maximized. In [9], Park and Hong analyzed the theoretical upper bound on the maximum achievable throughput of the energy harvesting based secondary user as a function of the energy arrival rate and the temporal correlation of the primary traffic under an energy causality and collision constraints. The fundamental trade-off between spectrum sensing and the SU expected throughput for a conventional energy unconstrained CRN is studied in [10]. Inspired by [10], Yin *et al.* [11] focused on the harvesting-sensing-throughput trade-off and the joint optimization for save-ratio (i.e. the proportion of the frame length expended on harvesting energy, denoted as $\rho : 0 \leq \rho < 1$), sensing duration, sensing threshold and fusion rule to maximize the expected throughput in the EH-CRN. The work in [12] jointly optimizes energy harvesting and spectrum sensing in the EH-CRN subject to the constraints on the energy causality, collision, and temporal correlation of probability of sensing the idle/occupied channel to maximize the achievable throughput. In [13], Khoshabi Nobar *et al.* investigate the performance of an RF-powered green cognitive radio network (RF-GCRN), where a central node, called a power beacon (PB), harvests green energy from ambient sources and wirelessly delivers random harvested energy to cognitive users. Nevertheless, [6]–[9], [11]–[13] merely address a non-cooperative spectrum sensing where a single SU co-exits with only one PU on the channel.

Biswas *et al.* [14] however, investigated a sensing-throughput optimization problem in EH-CRN based on cooperative spectrum sensing among the participating SUs. In particular, the authors focused on the trade-off between sensing time and sum capacity of the SUs with respect to transmission power and sensing time. In [15], Celik *et al.* considered the design of a heterogeneous energy efficient and energy harvesting cooperative spectrum sensing (EEH-CSS) scheme subject to the fundamental EEH-CSS constraints. The authors considered the heterogeneity of the SUs in terms of the non-identical harvesting, sensing, and reporting characteristics. The problem in [15] is formulated to determine the optimal asymptotic active probability, sensing duration, and detection threshold that maximize the achievable total throughput. The study in [14] formulated the problem as a mixed integer non-linear program (MINLP) with the objective to determine the access decision variables, the transmit power, the optimal sensing time and the number of slot that maximize the average throughput. In [16], Pratibha *et al.* employ the finite-horizon POMDP model to derive the optimal policy that can maximize the expected throughput while satisfying the PU detection and the energy causality constraints. The study in [17] optimizes the optimal sensing time that maximizes average throughput and the harvested energy. In [18], for an overlay EH CRN, the authors aim to find an optimal sensing time to maximize throughput of SU and the harvested RF energy. Residual energy maximization is explored with spectrum sensing and SU transmission in [19].

The critical issue in EH-CRN from the afore-mentioned literature is that the RF energy arrival from the ambient RF is random, while the magnitude of the electrical energy derived from the harvested RF may not always be sufficient to maximize throughput. The works in [15] and [20] considered a hybrid energy harvesting network model where the secondary user is capable of harvesting energy from both renewable sources (e.g. solar) and ambient radio frequency signals. However, the concern with this is that the application of such conventional renewable energy could be limited in certain environments, time and weather and, this could be critical in applications where quality of service is of utmost concern. In [21], the SU splits the channel into two sub-channel sets. One for sensing the PU and the other for collecting the RF of the PU signal. In the transmission slot, the harvested energy is supplied to compensate the sensing energy loss in order to guarantee the throughput. The problem is formulated to determine the optimal sub-channel set, sensing time, and transmission power that maximize the aggregate throughput, harvested energy and the energy efficiency of the SU over all the sub-channels. However, the details of the energy source for data transmission is not mentioned. In [22], RF energy could be harvested from the PU and the reporting SUs, and the problem is formulated into a multi-objective optimization (MOP) to optimize the spectrum sensing performance, under the constraints of the harvested energy at SU and the interference from SU on PU receiver. The afore-mentioned works only investigate a single channel case, which is quite simplistic for communication systems. Practical wireless communication networks are inherently multi-user and multichannel with peculiar challenges and benefits.

The authors in [23]–[25] propose a multi-channel harvesting schemes where an SU can sense the spectrum to determine the harvesting and communication geographical zones, such that it can take a decision to harvest or transmit data based on the zone it belongs to. An SU requiring to transmit data would need to stay in at least one of harvesting zones of active PUs, otherwise the SU will have no energy for transmitting data. In [24] the problem is formulated to jointly optimize the number of sensing samples and sensing threshold in order to minimize the sensing time and hence maximize the harvested energy. Xu *et al.* [25] investigated the problem to determine the optimal channel selection probability that

maximizes the average throughput of SUs. In these papers, cooperative spectrum sensing is not considered.

Optimal multi-channel cooperative spectrum sensing in energy unconstrained CRN has been studied in [26], where the authors formulated the problem to determine the optimal sensing time in a slot and how the total sensing time can be distributed to all channels. However, for energy harvesting system, the sensing-throughput trade-off that naturally exits in a conventional CRN is further complicated by energy constraint. Nevertheless, inspired by [26], the work presented in this paper focuses on finding the optimal cooperative spectrum sensing parameters in multi-channel cognitive radio networks with energy harvesting. In addition, the work presented here also investigates a different network scenario from the study in [26], in terms of the channel assignment to each user. In what follows, the main contributions of this paper are summarized.

B. MAIN CONTRIBUTIONS

1) Different from the studies on EH-CRNs, which focus on single channel network model [14], [15], the work presented in this paper considers the performance of energy harvesting secondary users in a practical multi-channel environment. In order to enhance the spectrum sensing performance, the secondary networks (SN) is modeled as overlapping clusters, where the number and the candidate channels assigned to each user are not necessarily equal. In addition, the heterogeneity of the network is also considered in terms of sensing quality of the cooperating secondary users.
2) The performance of the EH-CRNs in terms of the achievable throughput has been reported to be dependent on the energy arrival rate [6], [9]. This paper shows that by exploiting the benefit of the multi-channel scenario, the amount of energy harvested can increase with increasing number of the assigned channels to each SU. This improves the probability that the SU is active and correspondingly improves throughput. However, this is not without a cost, since energy consumption also increases with the number of channels sensed, revealing that there is an optimum number of PU channels to SU which, maximizes the energy efficiency of the EH-CRN.
3) With a goal to maximize the average throughput of the energy harvesting based SUs, the problem is formulated as a mixed integer non-linear optimization problem (MINLP) to jointly determine the optimal channel assignment, sensing duration in each frame, distribution of the sensing duration among the assigned channels for every SUs, and the detection threshold of each SU sensing each channel. This differs from [14], [15] and [26], in that while [14] and [15] only considered the problem in a single channel EH-CRN, the authors in [26] investigated the problem in a conventional (energy unconstrained) CRN, where a set of SUs are made to sense the same group of PU channels.

II. SYSTEM MODEL

This section describes the model and assumptions adopted for the cooperative spectrum sensing in multichannel cognitive radio networks with energy harvesting

A. COGNITIVE RADIO NETWORK MODEL

This paper considers a cooperative spectrum sensing in multichannel cognitive radio networks with energy harvesting secondary users. The network comprises N SUs and M PUs, both randomly deployed within Am^2 area. The distance between PUj and SUi is denoted as $d_{i,j}^{sp}$ whereas the distance between SUi and SUk ($i \neq k$) is $d_{i,k}^{ss}$. Both $d_{i,j}^{sp}$ and $d_{i,k}^{ss}$ are random values, since the deployment of both PUs and SUs are assumed random. The secondary users' network includes a central controller (CC) located within the transmission range of the SUs. The CC gathers the individual SU parameters such as the evaluated non-cooperative probability of miss-detection, the channel list, and the co-ordinates of the SUs locations. The CC is responsible for the frequency assignment based on the received information from the SUs. Therefore, the frequency assignment is done centrally, while cooperative spectrum sensing for channel access is distributed since SUs in each cluster cooperatively decide the status of each channel.

The considered time slotted operation of active energy harvesting based secondary users (EH-SUs) with heterogeneous SNR is illustrated in Figures 1a and 1b, in which cluster formation (or channel assignment) precedes the sensing-transmission/ harvesting frame. The frame length T is divided into a sensing period with duration τ_s, the reporting/data fusion/broadcasting time of τ_r and the transmission/harvesting period of $t_T = T - \tau_s - \tau_r$. During the sensing phase, each SU executes local spectrum sensing of the assigned K channels within period τ_s based on energy detection method. The SUs then report the sensing results to the corresponding cluster heads in each of the K clusters for cooperative decision. Each SU is updated with the channel status by the cluster heads through broadcast. It is assumed that the secondary user network is scheduled to transmit on time division multiple access (TDMA) protocol. Therefore, the transmission period in each frame is further divided into (data transmission) slots, and each SU i is allocated a slot $t_{i,j}$ on its transmit channel j, which is equivalent to

$$t_{i,j} = \frac{(T - \tau_r - \tau_s)}{z^j}, \quad \forall i \in \{1, 2, \cdots z^j\}, \tag{1}$$

where the parameter z^j denotes the number of SUs assigned to transmit on channel j.

Fig. 1a shows a scenario where each SU can opportunistically transmit or harvest RF energy from the PU of the transmit channel only. For instance, $SU1$ in the figure first cooperate with other SUs in all the K clusters to sense the PU channels in those K clusters. If the transmit channel is determined idle H_0^t, the SU would transmit its data in the transmission slot $S2$ and then sleep in the remaining period. However, if the transmit channel is busy H_1^t, the SU harvest

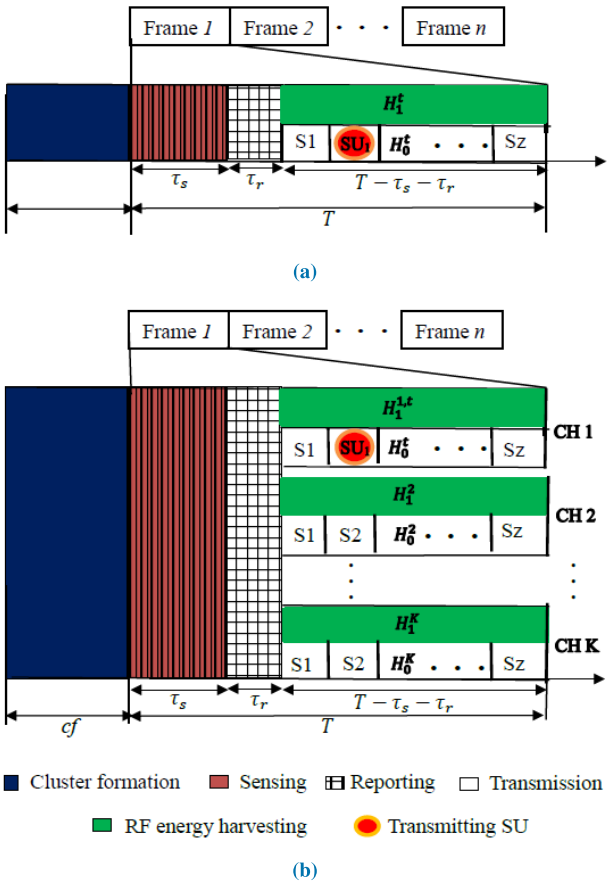

FIGURE 1. System model illustrating the frame structure of the cooperative spectrum sensing activities in EH-CRNs. Cluster formation precedes the sensing-transmission frame. Each frame is divided into z^j time slots ($S1, S2, \cdots Sz$), where z is the number of SUs allocated on channel j for opportunistic access: (a) single RF harvesting source (b) multiple RF harvesting sources.

RF energy from the PU throughout the period. It is assumed that channel status does not change within a frame. Fig. 1b on the other hand illustrates the scenario where SU can opportunistically harvest from multiple RF sources.

In Fig. 1b, after cooperative spectrum sensing to determine the channel status, $SU1$ harvest RF energy from the transmit channel ($CH1$) if the channel is busy $H_1^{1,t}$. If the channel is idle $H_0^{1,t}$, the SU transmits on slot 2 of $CH1$ and then harvest opportunistically from any of the $K-1$ (i.e. $2, \cdots, K$) channels for the remaining period. Fig. 2 illustrates the considered (overlapping) clusters, in which multiple channels are assigned to each SU, while each PU can cooperatively be sensed by multiple SUs. This is a case of many-to-many combinatorial assignment.

Therefore, a cluster is made up of a group of SUs that cooperate to sense a particular PU channel. In this case, an SU can belong to multiple clusters. Hence, all the SUs in a cluster may not necessarily share one channel for transmission in every frame. Following the channel assignment at the beginning of each frame, each SU selects one of the K assigned channels randomly as a transmit channel. It is assumed that

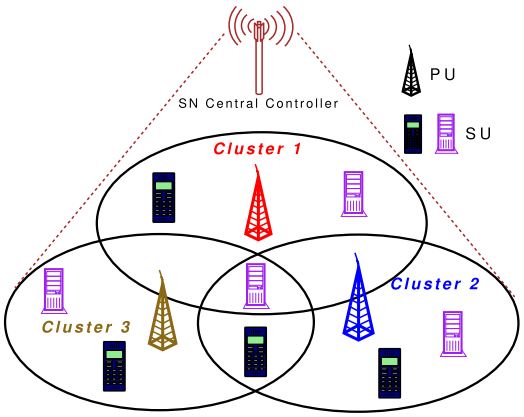

FIGURE 2. Network model illustrating overlap clustering assignment.

the energy requirement for cluster formation is negligible in comparison with the energy demand for spectrum sensing and data transmission, since the bulk of the cluster formation/channel assignment work is performed by the central controller.

B. PRIMARY NETWORK MODEL

A primary network (PN) with M narrow band spectrum (channels) is considered. The network equally comprises of M PUs that share these spectrum, such that each PU is licensed to one channel. The primary user traffic on each channel is modeled as a time homogeneous discrete Markov process as assumed for example in [15]. Therefore, the spectrum randomly alternates its states between the channel being vacant and occupied. If $S_{j,t}$ denotes the spectrum occupancy state of channel j on slot t, then the binary hypothesis of the channel status can be represented as $S_{j,t} \in \{0(vacant), 1(busy)\}$. The steady state probabilities of the channel being idle and busy are denoted as $P(H_0)$ and $P(H_1)$.

C. COOPERATIVE SPECTRUM SENSING

Spectrum sensing is executed during the sensing phase. The number of channels assigned to SU i (otherwise referred to as channel list) is denoted as K_i, where K_i ($1 \leq K_i \leq M$) is the number of channels assigned to SU i. The channel list may be different for different users. Each SU independently senses the assigned channels sequentially within the sensing period denoted by $\tau_s = \sum_{j=1}^{M} x_{i,j}\tau_{i,j}, \forall i = \{1, \ldots, N\}$, where $x_{i,j}$ is the assignment variable and $\tau_{i,j}$ denotes the sensing time of SU i on channel j. The sensing results are then reported to the corresponding head in each cluster through a dedicated common control channel (CCC) based on time-slotted scheme. Each cluster head makes a cooperative decision about the channel status and updates the SUs through broadcasts. Hence, SU i is updated with the cooperative sensing decisions of the K_i assigned channels from the respective cluster heads. Therefore, the work models a centralized channel assignment scheme for a distributed cooperative spectrum

sensing. The secondary users only exchange their sensing decisions with the cluster heads in the respective clusters for the cluster-based cooperative spectrum sensing.

Assuming a complex value PSK modulated signal and circularly symmetric complex Gaussian (CSCG) noise for primary signal and additive noise in the wireless channel, the probabilities of detection and false alarm as evaluated by SU i on channel j can be expressed as

$$P_{d,i,j} = Q\left(\left(\frac{\varepsilon_{i,j}}{\sigma_w^2} - \bar{\gamma}_{i,j} - 1\right)\sqrt{\frac{\tau_{i,j} f_s}{2\bar{\gamma}_{i,j} + 1}}\right) \tag{2}$$

$$P_{f,i,j} = Q\left(\left(\frac{\varepsilon_{i,j}}{\sigma_w^2} - 1\right)\sqrt{\tau_{i,j} f_s}\right) \tag{3}$$

where, $\varepsilon_{i,j}$, $\bar{\gamma}_{i,j}$, f_s and σ_w denote the detection threshold of SU i on channel j, the average SNR of channel j on SU i, the sampling frequency and the noise variance respectively. The probability of a miss-detection can be obtained from (2) as

$$P_{m,i,j} = 1 - P_{d,i,j} \tag{4}$$

The cooperative probability of detection and the cooperative probability of false alarm as computed by each cluster head for each channel based on OR decision fusion are evaluated as

$$Q_{D,j} = 1 - \prod_{i=1}^{N}\left(1 - P_{d,i,j}^{I}\right)^{x_{i,j}}, \quad \forall j = \{1, \cdots, M\} \tag{5}$$

$$Q_{F,j} = 1 - \prod_{i=1}^{N}\left(1 - P_{f,i,j}^{I}\right)^{x_{i,j}}, \quad \forall j = \{1, \cdots, M\} \tag{6}$$

where $P_{m,i,j}^{I} = P_{m,i,j}(1 - P_e) + (1 - P_{m,i,j})P_e$ and $P_{f,i,j}^{I} = P_{f,i,j}(1 - P_e) + (1 - P_{f,i,j})P_e$. The parameter P_e denotes the probability of reporting error. The OR rule is adopted as a decision fusion rule being the optimal rule to minimize interference to the primary user.

D. ENERGY MODEL

It is assumed that the SU can only perform either spectrum sensing followed by data transmission, or energy harvesting at a time. Therefore, the charging process must stop while the SU draws energy from the storage device to either sense the spectrum or transmit the data in its queue. The power consumption by each SU for spectrum sensing, cooperative spectrum sensing overhead and data transmission activities are denoted as p_s, p_r, and p_t respectively. The energy state of the SU storage facility (e.g. a super-capacitor) at the beginning of the n^{th} frame is denoted as $e_{i,n}$. Hence, SU cannot participate in the cooperative spectrum sensing when $e_{i,n} < (p_s\tau_s + p_r\tau_r)$.

It is assumed that secondary users harvest RF energy from the transmitting primary users. Nevertheless, the model can equally address a scenario where energy can be harvested from other sources in addition to the primary user RF. The maximum amount of energy that can be harvested in the n^{th} frame is expressed as:

$$e_{h,i,n} = P_{avail}\ t_T\ Pr(\varrho), \tag{7}$$

where $t_T = (T - \tau_s - \tau_r)$ is the maximum period available for energy harvesting in each frame. The parameter $P(\varrho)$ denotes the probability that there is an harvested RF energy, and $P_{avail} = P_R\ \eta_{H/C}$ represents the output of the secondary user harvesting circuit, which is defined as the product of the amount of received RF power P_R at the SU and the harvesting circuit efficiency $\eta_{H/C}$. The amount of harvested RF energy by secondary users therefore, depends on the magnitude of the received RF power, the harvesting circuit efficiency, the harvesting duration and the probability that an RF harvesting source is available.

The total energy consumption by SU i in the n^{th} frame denoted as $e_{c,i,n}$ can explicitly be expressed as

$$e_{c,i,n} = p_s\tau_s + p_r\tau_r + \Big\{P(H_0)(1 - Q_{F,j}) + P(H_1)(1 - Q_{D,j})\Big\} \times p_t\ t_T, \tag{8}$$

where the first, second and third expression on the RHS of (8) are the sensing energy, the reporting energy and transmission energy respectively. Parameters $P(H_0)$ and $P(H_1)$ are the probabilities that the transmit channel is vacant and occupied with PU signal respectively. When the harvested and consumed energy are both put into perspective, the residual energy (state) at the beginning of the next $(n+1)^{th}$ frame for an infinite energy storage capacity device can be updated as

$$e_{i,n+1} = max\{0, [e_{i,n} + e_{h,i,n} - e_{c,i,n}]\} \tag{9}$$

III. PROBLEM FORMULATION

In this section, two different scenarios are considered namely: *A*) single harvesting source where the SU can harvest only from the PU occupying the transmit channel, and *B*) multiple RF harvesting source in which the SU can opportunistically harvest from any of the PU in the assigned channels.

A. SINGLE RF ENERGY HARVESTING SOURCE

Under this scenario, the SU can only harvest from the elected transmit channel when occupied with a primary user signal. This model can also be used for EH-CRN with a single dedicated RF energy harvesting source. The possible energy states during the n^{th} frame are as follows

1) The channel correctly detected to be busy with probability $P(H_1)Q_{D,j}$. In this case, secondary user does not transmit, but can harvest energy from the transmitting primary user in the rest of the n^{th} frame. Therefore, the throughput is zero.
2) Channel correctly detected to be idle with probability $P(H_0)(1 - Q_{F,j})$. The SU transmits in the n^{th} frame for a period of $\frac{T-\tau_r-\tau_s}{z^j}$ and sleep for the rest of the frame. Energy harvested is zero.
3) Channel incorrectly detected to be busy (false alarm) with probability $P(H_0)Q_{F,j}$. The SU's opportunity to

$$
\begin{aligned}
e^{s,1}_{h,i,n} &= P_{avail} t_T P(H_1), \quad e_{c,i,n} = p_s\tau_s + p_r\tau_r \quad : P(H_1)Q_{D,j} \\
e^{s,0}_{h,i,n} &= 0, \quad e_{c,i,n} = p_s\tau_s + p_r\tau_r + p_t\left(\frac{t_T}{z^j}\right) \quad : P(H_0)(1-Q_{F,j}) \\
e^{s,0}_{h,i,n} &= 0, \quad e_{c,i,n} = p_s\tau_s + p_r\tau_r \quad : P(H_0)Q_{F,j} \\
e^{s,1}_{h,i,n} &= 0, \quad e_{c,i,n} = p_s\tau_s + p_r\tau_r + p_t\left(\frac{t_T}{z^j}\right) \quad : P(H_1)(1-Q_{D,j})
\end{aligned} \tag{10}
$$

$$
e^{s}_{i,n+1} = \begin{cases} e_{i,n} + e^{s,1}_{h,i,n} - p_s\tau_s - p_r\tau_r & : P(H_1)Q_{D,j} \\ e_{i,n} - p_s\tau_s - p_r\tau_r, & : P(H_0)Q_{F,j} \\ e_{i,n} - p_s\tau_s - p_r\tau_r - p_t\left(\frac{t_T}{z^j}\right) & : P(H_0)(1-)Q_{F,j}) + P(H_1)(1-Q_{D,j}) \end{cases} \tag{11}
$$

access the channel is lost. No energy is harvested and the achievable throughput is also zero.

4) Channel incorrectly detected to be vacant (miss-detection) with probability $P(H_1)(1-Q_{D,j})$. The SU transmits in the n^{th} frame, but the data interferes with the primary user's signal, and nothing is gained.

Therefore, under this scenario, the SU can harvest energy on the transmit channel with probability $P(H_1)Q_{D,j}$, transmit data with probability $P(H_0)(1-Q_{F,j}) + P(H_1)(1-Q_{D,j})$, or remain idle (neither harvesting RF nor transmitting) with probability $P(H_0)Q_{F,j}$. The amount of energy consumed and energy harvested $e^{s,\mu}_{h,i,n}$ (where, $\mu \in \{0,1\}$ denotes the channel's idle and busy status respectively) in each state can be expressed as in (10), as shown at the top of this page. While an action is taken, the SU energy state in the next frame is evaluated as (11), as shown at the top of this page. Therefore, from (10) the amount of harvested energy in a single source scenario can be expressed as

$$
e^{s}_{h,i,n} = P_{avail} \cdot t_T \cdot P(\varrho^s), \tag{12}
$$

where $P(\varrho^s) = P(H_1)$.

B. MULTIPLE RF ENERGY HARVESTING SOURCES

This is particularly useful in a network where primary user services may be inactive for a long period of time (e.g., digital TV broadcasting), and the stored energy in the SUs would more likely get depleted resulting in outages. The possible states during the n^{th} frame are:

1) The transmit channel correctly detected to be busy with probability $P(H_1)Q_{D,j}$. In this case, secondary user does not transmit, but can harvest energy in the rest of the n^{th} frame. Therefore, the throughput is zero.
2) Transmit channel correctly detected to be idle with probability $P(H_0)(1-Q_{F,j})$. The SU transmits in the n^{th} frame for a period $t_{i,j}$ (as defined in (1)) and can then harvest from any of the $K_i - 1$ channels that is found busy for the rest of the frame.
3) Transmit channel incorrectly detected to be busy (false alarm) with probability $P(H_0)Q_{F,j}$. The SU's opportunity to access the channel is lost. The achievable throughput is therefore zero, and no energy is harvested.
4) Transmit channel incorrectly detected to be vacant (miss-detection) with probability $P(H_1)(1-Q_{D,j})$. The SU transmits in the n^{th} frame, but the data interferes with the primary user's signal, and nothing is gained. However, energy can be harvested from any of the $K_i - 1$ channels for the rest of the frame.

Therefore, different from the single harvesting source scenario, the SU can opportunistically harvest energy in every frame except when there is a false alarm on the transmit channel. The amount of energy consumed and harvested in each state can be expressed as in (13), as shown at the top of the next page. When an action is taken, the SU energy state in the next frame can similarly be expressed as (14), as shown at the top of the next page. The parameter $P(\Omega_1)$ is the steady state probability that at least one of the remaining $K_i - 1$ assigned channels would be occupied by PU and thus be available for energy harvesting by the SU. This probability follows a *binomial* distribution given as

$$
Pr(\Omega_1) = \sum_{j=1}^{K_i-1} \binom{K_i-1}{j} Pr(H_1)^j (1-Pr(H_1))^{K_i-1-j}, \tag{15}
$$

where

$$
\binom{K_i-1}{j} = \frac{(K_i-1)!}{(K_i-1-j)!j!}. \tag{16}
$$

From (13), the amount of harvested energy in the multiple harvesting sources scenario can be expressed as

$$
e^{m}_{h,i,n} = P_{avail} t_T \cdot P(\varrho^m), \tag{17}
$$

where $P(\varrho^m) = \min\left(1, \left(P(H_1) + P(\Omega_1)\left(\frac{z^j-1}{z^j}\right)\right)\right)$ is the probability of energy harvesting in a multiple source scenario. At $K_i = 1$, the expression in (17) becomes $e^{m}_{h,i,n} = e^{s}_{h,i,n}$ since there is no event to choose from, making $Pr(\Omega_1) = 0$. Therefore, the multichannel gain on the harvested energy (i.e. the ratio of the harvested energy in a multiple harvesting source to the harvested energy in a single harvesting source)

$$
\begin{aligned}
e^{m,1}_{h,i,n} &= P_{avail}\cdot t_T P(H_1), \quad e_{c,i,n} = p_s\tau_s + p_r\tau_r && : P(H_1)Q_{D,j}\\
e^{m,0}_{h,i,n} &= P_{avail}\frac{(z^j-1)(t_T)}{z^j}P(\Omega_1), \quad e_{c,i,n} = p_s\tau_s + p_r\tau_r + p_t\left(\frac{t_T}{z^j}\right) && : P(H_0)(1-Q_{F,j})\\
e^{m,0}_{h,i,n} &= 0, \quad e_{c,i,n} = p_s\tau_s + p_r\tau_r && : P(H_0)Q_{F,j}\\
e^{m,1}_{h,i,n} &= P_{avail}\frac{(z^j-1)(t_T)}{z^j}P(\Omega_1), \quad e_{c,i,n} = p_s\tau_s + p_r\tau_r + p_t\left(\frac{t_T}{z^j}\right) && : P(H_1)(1-Q_{D,j})
\end{aligned} \tag{13}
$$

$$
e^{m}_{i,n+1} = \begin{cases}
e_{i,n} + P_{avail}t_T\cdot P(H_1) - p_s\tau_s - p_r\tau_r & : P(H_1)Q_{D,j}\\
e_{i,n} - p_s\tau_s - p_r\tau_r, & : P(H_0)Q_{f,j}\\
e_{i,n} + P_{avail}\frac{(z^j-1)(t_T)}{z^j}P(\Omega_1) & \\
\quad - p_s\tau_s - p_r\tau_r - p_t\left(\frac{t_T}{z^j}\right) & : P(H_0)(1-Q_{F,j}) + P(H_1)(1-Q_{D,j})
\end{cases} \tag{14}
$$

can be evaluated as

$$
G^m_{h,i,n} = \frac{e^m_{h,i,n}}{e^s_{h,i,n}} = \frac{P(\varrho^m)}{P(\varrho^s)}, \tag{18}
$$

where the expression in (18) is upper bounded as $P(H_1)^{-1}$.

In both cases considered in Sections III-A and III-B, the EH-CRN results in a dynamic secondary user energy state over time, and the energy level in the $(n+1)^{th}$ frame depends on the residual energy and the action taken during the n^{th} frame. The design strategy for the EH-CRN can thus be formulated as a stochastic optimal control problem given by $\pi^* = arg\max_{\pi} V^{\pi}(S_0)$, and the expected reward is defined as [27]

$$
V^{\pi}(s_0) = arg\max_{\pi}\mathbb{E}\left[\sum_{r=1}^{G}\delta^{r-1}R(s_r, a_r)\right], \tag{19}
$$

where $0 < \delta < 1$ is a discount factor that trades off the importance of the immediate and future reward. The target is to determine the optimal policy π which specifies the optimal action in the state and maximizes the long-term expected reward. The policy π therefore, maps the SU energy state at each frame to the possible action taken, while G represents the planning horizon. Therefore, (19) models a general class of Markov decision processes (MDP), in which states $\{s_1, \cdots s_G\} \in S$ refer to the SU energy states, and the action $\{a_1 \cdots a_G\} \in A$ refers to the amount of energy to be used for spectrum sensing and data transmission. The optimal value function V^{π^*} of policy π represents the maximum cumulative function of rewards (i.e. $V^{\pi^*} \geq V^{\pi}$) which can be obtained as a solution of the Bellman recursion, given by

$$
\begin{aligned}
V_n(S) &= \max_{a\in A}\mathbb{E}\left[R(s) + \delta\sum_{s'\in S}T(s,a,s')V_{n-1}(s')\right]\\
&= \max_{a\in A}\mathbb{E}\Bigg[\frac{t_T}{T}\Bigg\{(1-Q_{F,j})P(H_0)C_{0,j}\\
&\quad + (1-Q_{D,j})P(H_1)C_{1,j}\\
&\quad + \delta\sum_{s'\in S}\left(P(H_0)(1-Q_{F,j}) + P(H_1)(1-Q_{D,j})\right)\\
&\quad \times\left(e_{i,n} - p_s\tau_s - p_r\tau_r - p_t\left(\frac{t_T}{z^j}\right) + \beta_{h,i,n}\right)\\
&\quad + P(H_1)Q_{D,j}\left(e_{i,n} + \phi_{h,i,n} - p_s\tau_s - p_r\tau_r\right)\\
&\quad + P(H_0)Q_{F,j}\left(e_{i,n} - p_s\tau_s - p_r\tau_r\right)\Bigg\}\Bigg],
\end{aligned} \tag{20}
$$

The parameter $\phi_{h,i,n}$ represents the energy harvested when the transmit channel is correctly detected to be busy (as expressed in both (10) and (13)). The parameter $\beta_{h,i,n}$ represents the energy harvested from any of the $K_i - 1$ channels, which is zero for $K_i = 1$, whereas $T(s,a,s') = Pr(s'|s,a)$ is the transition function, which expresses the probability that the SU energy state changes from s' to s when action a is taken.

However, the state and action space in (19) for EH-CRN are continuous and infinite, making the solution computationally intractable, more especially for the multi-user, multi-channel case under consideration. Hence, in the subsequent section, the impact of the current action on the future reward will be ignored, and focus only on maximizing the expected immediate reward in an optimal myopic strategy. This approximation method is also adopted in the works presented in [11] and [15] among others.

IV. APPROXIMATE FORMULATION AND SOLUTION

Optimizing the original problem in (20) is a sequential decision making process which attempts to determine the immediate and future rewards based on the possible actions taken. However, this becomes very difficult due to the tight coupling between the current action and the future reward. In this section, the original stochastic optimal control problem is approximated to a myopic policy such that the optimal policy in (20) can be approximated as

$$
\begin{aligned}
V_n(S) &\approx R(x_{i,j}, \tau_s, \tau_{i,j}, \varepsilon_j)\\
&= \frac{(T-\tau_s-\tau_r)}{T}\Bigg\{(1-Q_{F,j})P(H_0)C_{0,j}\\
&\qquad + (1-Q_{D,j})P(H_1)C_{1,j}\Bigg\},
\end{aligned} \tag{21}
$$

where (21) is the immediate reward on channel j based on the current action, the parameter $C_{0,j} = \log_2(1 + \xi_{i,j})$ represents the average capacity of the SU i on the idle channel j, and $C_{1,j} = \log_2(1 + \frac{\xi_{i,j}}{1+\xi_j})$, denotes the capacity of the SU i when there is collision with the primary user signal (with SNR ξ_j) due to miss-detection. Since SUi can only select one of the K_i channels randomly as a transmit channel, a mean value of $\xi_{i,j} = \bar{\xi}^s$ and $\xi_j = \bar{\xi}^p$ are assumed for SNR values of SU and PU on the transmit channel. Hence, the average capacity of the SU on the transmit channel without or with the presence of PU signal can be expressed as $C_0 = \log_2(1 + \bar{\xi}^s)$ and $C_1 = \log_2(1 + \frac{\bar{\xi}^s}{1+\bar{\xi}^p})$ respectively. Different from the solution to the problem in (20), this policy is essentially a static approach. Existing studies have however shown that myopic policy is close in performance to the optimal policy [28]–[30].

The objective is to jointly determine the optimal channel assignment ($x_{i,j}$), the detection threshold ($\varepsilon_{i,j}$), the sensing duration (τ_s), and the distribution of the sensing duration among the assigned channels ($\tau_{i,j}$). This is done with a goal to maximize the average throughput of the secondary users. The time taken by SU i to sense channel j, $j \in \{1, 2, .., M\}$ is denoted by $\tau_{i,j}$, $i \in \{1, 2, \ldots, N\}$, and both τ_s and $\tau_{i,j}$ are continuous variables. The average normalized throughput maximization per channel can thus be formulated as

Problem P1:

$$\begin{aligned}\max_{\tau_s,\{\tau_{i,j}\},\{\varepsilon_{i,j}\},\{x_{i,j}\}} \; & R(\tau_s, \tau_{i,j}, \varepsilon_{i,j}, x_{i,j}) \\ &= \max_{\tau_s,\{\tau_{i,j}\},\{\varepsilon_{i,j}\},\{x_{i,j}\}} \Bigg[\frac{T-\tau_s-\tau_r}{TM} \\ &\times \sum_{j=1}^{M} \Big((1 - Q_{F,j}(\tau_{i,j}, \varepsilon_{i,j}, x_{i,j}))P(H_0)C_{0,j} \\ &+ (1 - Q_{D,j}(\tau_{i,j}, \varepsilon_{i,j}, x_{i,j}))P(H_1)C_{1,j}\Big)\Bigg], \end{aligned} \tag{22}$$

$$\text{subject to: } Q_{D,j}(\tau_{i,j}, \varepsilon_{i,j}, x_{i,j}) \geq \beta, \tag{C1}$$

$$e_{c,i,n} \leq \bar{e}_{h,n}, \quad i \in \{1, \ldots, N\}, \tag{C2}$$

$$0 \leq \tau_s \leq (T - \tau_r), \tag{C3}$$

$$\sum_{j=1}^{M} x_{i,j}\tau_{i,j} = \tau_s, \quad \tau_{i,j} > 0, \ \forall i \in \{1, \ldots, N\}, \tag{C4}$$

$$\sum_{j=1}^{M} x_{i,j} \leq K_{max}, \quad \forall i \in \{1, \ldots, N\}, \tag{C5}$$

$$\sum_{j=1}^{N} x_{i,j} \leq n_{max}, \quad \forall j \in \{1, \ldots, M\}, \tag{C6}$$

$$x_{i,j} \in \{0, 1\}, \tag{C7}$$

where

$$\begin{aligned}\bar{e}_{c,i,n} &= p_s\tau_s + p_r\tau_r \\ &+ \frac{T-\tau_r-\tau_s}{M} p_t \sum_{j=1}^{M} \Big(P(H_0)(1 - Q_{F,j}) \\ &+ P(H_1)(1 - Q_{D,j})\Big).\end{aligned}$$

In problem P1, the expression in (22) defines the objective function. Constraint (C1) guarantees the protection of PU against interference from SUs, while (C2) and (C3) ensure that the energy causality and time causality are satisfied. The constraints in (C2) and (C3) guarantee that the average energy budget of the SU does not exceed its total available energy and that the time budget does not exceed the frame period respectively. Constraint (C4) ensures that the total time spent by any SU in sensing the assigned channels K_i, ($1 \leq K_i \leq M$) does not exceed the sensing duration τ_s in a frame. In constraints (C5) and (C6), the number of PU channels that can be assigned to any SU, and the number of SUs that can be assigned to a single PU channel are limited to a specified values. Constraint (C7) defines the assignment variable type. From constraints (C5) and (C6), the assignment problem defines an overlapping cluster scheme, where an SU can belong to multiple clusters. Each cluster is however, identified with a particular channel or frequency.

The problem in P1 is a mixed integer non-linear optimization (MINLP) and non-convex jointly in $x_{i,j}$, τ_s, $\tau_{i,j}$, and $\varepsilon_{i,j}$. The problem defines a more complicated scenario due to the consideration for a practical overlapping clustered network in the multi-channel scenario. High degree of coupling also exists among the optimization variables, which makes direct decomposition difficult. In order to solve it, the approach of alternating convex optimization is adopted [31]. That is, given a non-convex problem $f(x)$ with variables $(x_1, \ldots x_n) \in \mathbb{R}^n$, while $t_1, \ldots, t_k \subset \{1, \ldots n\}$ are index subsets with $t_j \in \{1, \ldots, n\}$, and supposing the problem is convex in subset of variables x_i, $i \in t_j$, then alternating convex optimization method involves cycling through j, in each step optimizing over variable x_i while, $i \notin t_j$ are fixed [32]. Hence, the procedure alternates between determining the optimal assignment $x_{i,j}$ with fixed τ_s, $\varepsilon_{i,j}$, and $\tau_{i,j}$, and then, given $x_{i,j}$, with fixed $\varepsilon_{i,j}$ and $\tau_{i,j}$, optimize over τ_s. Finally, with given $x_{i,j}$ and τ_s optimize over $\tau_{i,j}$, and $\varepsilon_{i,j}$, and vice-versa iteratively until the algorithm converges.

A. OPTIMAL CHANNEL ASSIGNMENT

With fixed values of τ_s, $\varepsilon_{i,j}$, and $\tau_{i,j}$, problem P1 reduces to a channel assignment problem. Furthermore, for a fixed sensing budget in terms of the time-bandwidth product in the energy detection-based sensing scheme, the sensing performance is an increasing function of the received signal-to-noise-ratio. Therefore, by taking SNR as an active parameter for determining the optimal channel assignment, the first expression in the RHS of the objective function in (22) reduces to a constant term since the probability of false

alarm (2) is independent of SNR. Moreover, in the overlay CRN under consideration, the secondary users cannot have a successful transmission when the channel is occupied with the PU signal. Therefore, it is only reasonable to minimize the second expression on the RHS of the objective function in problem P1, (i.e. $(1-Q_{D,j})P(H_1)C_{1,j}$) in order to reduce interference to PU signal and the energy consumption for unsuccessful transmission. This is equivalent to

Problem P2:

$$\max_{\chi} Z(x_{i,j}, \tau_s, \tau_{i,j}, \varepsilon_{i,j}) = \min_{\chi} \sum_{j=1}^{M} \left\{1 - Q_{D,j}(x_{i,j})\right\}, \quad (23)$$

$$\text{subject to}: \sum_{i=1}^{N} x_{i,j} \leq n_{max},\ j \in \{1,2,\ldots,M\}, \quad (C1)$$

$$\sum_{j=1}^{M} x_{i,j} \leq K_{max},\ i \in \{1,2,\ldots,N\}, \quad (C2)$$

$$x_{i,j} \in \{0,1\}. \quad (C3)$$

The assignment matrix is represented by $\chi = \{x_{i,j}\}_{M\times N}$, that is $x_{i,j} = 0$ or 1 depending on whether SU i is assigned channel j or not. The problem in (23) is a nonlinear integer programming problem. However, by substituting (5) into (23), and then using the identities $min(.) \equiv min\ log_e(.)$ and $log_e \prod(.) = \sum log_e(.)$, the objective function in (23) can be linearized, such that problem P2 can otherwise be expressed as a linear problem as follows

Problem P3:

$$\max_{\chi} Z(\chi, \tau_s, \tau_{i,j}, \varepsilon_{i,j}) = \min_{\chi} \sum_{j=1}^{M}\sum_{i=1}^{N} x_{i,j} log_e \left\{P^I_{m,i,j|\gamma_{i,j}}\right\} \quad (24)$$

$$\text{subject to}: \sum_{i=1}^{N} x_{i,j} \leq n_{max},\ j \in \{1,2,\ldots,M\}, \quad (C1)$$

$$\sum_{j=1}^{M} x_{i,j} \leq K_{max},\ i \in \{1,2,\ldots,N\}, \quad (C2)$$

$$x_{i,j} \in \{0,1\}, \quad (C3)$$

where $P_{m,i,j|\gamma_{i,j}}$ is the non-cooperative probability of miss-detection based on outdated channel state information [33], evaluated as

$$P_{m,i,j|\gamma_{i,j}} \approx 1 - exp\left(-\frac{\varepsilon_{i,j}}{2} - \frac{\gamma_{i,j}\rho^2_{i,j}}{\bar{\gamma}_{i,j}(1-\rho^2_{i,j})}\right) \times \sum_{k=0}^{L} \frac{\left\{\bar{\gamma}_{i,j}(1-\rho^2_{i,j})\right\}^k}{\left\{\bar{\gamma}_{i,j}(1-\rho^2_{i,j})+1\right\}^{k+1}} \sum_{q=0}^{u+k-1} \frac{1}{q!}\left(\frac{\varepsilon_{i,j}}{2}\right)^q \times {}_1F_1\left(-k, 1; -\frac{\gamma_{i,j}\rho^2_{i,j}}{\bar{\gamma}_{i,j}(1-\rho^2_{i,j})\left\{\bar{\gamma}_{i,j}(1-\rho^2_{i,j})+1\right\}}\right). \quad (25)$$

The motivation for (25) is to compensate for the independence of the PU activities and the effect of small scale fading during the channel assignment. The parameter $\gamma_{i,j}$ represents the instantaneous SNR of PU j at SU i, and $\bar{\gamma}_{i,j}$ denotes the average SNR of PU j at SU i. The parameter $\rho_{i,j} = J_0(2\pi F^{max}_{d,i,j}\epsilon_{i,j})$ is the correlation coefficient between the predicted channel response $\hat{h}_{i,j}$ and the outdated channel response $h_{i,j}$ (based on Jakes' correlation model), $J_0(.)$ is the Bessel function of the first kind and zeroth order, and $F^{max}_{d,i,j}$ denotes the maximum Doppler shift. Therefore, $\hat{h}_{i,j}$ and $h_{i,j}$ represent the channel responses at time $t+\epsilon_{i,j}$, and the outdated channel response at t respectively.

Equation (25) is however, a generalized expression for the probability of miss-detection in a practical channel. The case where the SU might only have access to causal CSI (which is equivalent to $\epsilon_{i,j} = 0$) is already embedded. Since, as $\rho^2_{i,j} \to 1$, which happens when $\epsilon_{i,j} \to 0$ or in a properly correlated channel, $P_{m,i,j|\gamma_{i,j}} \to 1 - Q_u\left(\sqrt{2\bar{\gamma}_{i,j}}, \sqrt{\varepsilon_{i,j}}\right)$ [33]. On the other hand, as $\rho^2_{i,j} \to 0$, i.e., with increasing $\epsilon_{i,j}$, (25) approaches

$$\hat{P}_{m,i,j} \approx 1 - \sum_{k=0}^{L} \frac{\left\{\bar{\gamma}_{i,j}\right\}^k}{\left\{\bar{\gamma}_{i,j}+1\right\}^{k+1}} exp\left(\frac{\varepsilon_{i,j}}{2}\right) \sum_{q=0}^{u+k-1} \frac{1}{q!}\left(\frac{\varepsilon_{i,j}}{2}\right)^q \quad (26)$$

where $\hat{P}_{m,i,j}$ is the average probability of miss-detection over Rayleigh fading without CSI.

Problem P3 is thus a linear integer programming, that describes a generalized assignment problem (GAP) with overlapping clusters (since $1 \leq K_i \leq K_{max}$). By defining another variable y_j as the value of the cooperative probability of miss-detection in each cluster, the linear integer problem in problem P3 can then be written as follows

Problem P3B:

$$Z(\chi, \boldsymbol{y}) = \min_{\chi, y_j} \sum_{j=1}^{M} y_j \quad (27)$$

$$\text{subject to}: \sum_{i=1}^{N} x_{i,j} \leq n_{max}, \quad j \in \{1,2,\ldots,M\} \quad (C1)$$

$$\sum_{j=1}^{M} x_{i,j} \leq K, \quad i \in \{1,2,\ldots,N\} \quad (C2)$$

$$\sum_{i=1}^{N} x_{i,j}\psi_{i,j} = y_j, \quad j \in \{1,2,\ldots,M\} \quad (C3)$$

$$x_{i,j} \in \{0,1\}, \quad y_j \in \Re \quad (C4)$$

where,

$$\psi_{i,j} = log_e\{P_{m,i,j|\gamma_{i,j}}(1-P_e) + (1-P_{m,i,j|\gamma_{i,j}})P_e\}$$

If the equality constraint in (C3) of P3B is relaxed and replaced by an inequality, then the problem in P3B can be

written as P3C following some algebraic manipulations and vectorization [36]

Problem P3C:

$$\min_{z} (0 \;\; C^T)z \tag{28}$$

$$\text{subject to}: \; (A_j \;\; 0)z \leq n_{max}, \quad j \in 1, \ldots, M \tag{C1}$$

$$(Q_i \;\; 0)z \leq K, \quad i \in 1, \ldots, N \tag{C2}$$

$$(\psi_j \;\; C_i)z \leq 0, \quad j \in 1, \ldots, M \tag{C3}$$

$$x_{i,j} \in \{0, 1\}, \quad y_j \in \Re \tag{C4}$$

where $z = \begin{pmatrix} \boldsymbol{x} \\ \boldsymbol{y} \end{pmatrix}$ and A_j, Q_i, and C_i represent the coefficient of the assignment variables define as

$$A = \left[I_m^{(1)}, \cdots, I_m^{(n)} \; 0_m \right]$$

$$Q = \left[\begin{array}{ccc:ccc:c:ccc:ccc} 1 & \cdots & 1 & 0 & \cdots & 0 & & 0 & \cdots & 0 & 0 & \cdots & 0 \\ 0 & \cdots & 0 & 1 & \cdots & 1 & & 0 & \cdots & 0 & 0 & \cdots & 0 \\ 0 & \cdots & 0 & 0 & \cdots & 0 & \cdots & 0 & \cdots & 0 & 0 & \cdots & 0 \\ \vdots & \ddots & \vdots & \vdots & \ddots & \vdots & & \vdots & \ddots & \vdots & \vdots & \ddots & \vdots \\ 0 & \cdots & 0 & 0 & \cdots & 0 & & 1 & \cdots & 1 & 0 & \cdots & 0 \end{array}\right]$$

$$C = \left[\psi I_m^{(1)}, \cdots, \psi I_m^{(n)} \; -I_m \right]$$

By concatenating the constraints (C1) - (C3) in problem P3C in the form

$$P = \begin{pmatrix} A_1 & 0 \\ \vdots & \vdots \\ A_M & 0 \\ Q_1 & 0 \\ \vdots & \vdots \\ Q_N & 0 \\ \psi_1 & C_1 \\ \vdots & \vdots \\ \psi_M & C_M \end{pmatrix}, \quad R = \begin{pmatrix} n_{max} \\ \vdots \\ n_{max} \\ K \\ \vdots \\ K \\ 0 \\ \vdots \\ 0 \end{pmatrix}$$

the problem in P3C can simply be written as

Problem P3D:

$$\min_{z} \bar{c}^T \boldsymbol{y} \tag{29}$$

$$\text{subject to}: \; Pz \leq R \tag{C1}$$

$$x_{i,j} \in \{0, 1\}, \quad y_j \in \Re \tag{C2}$$

where $\bar{c}^T = (0 \;\; C^T)$.

The solution to problem P3D follows a similar pattern as in [37], using the solver from the optimization toolbox provided by MATLAB which is designed to solve a similar mixed integer linear problem (MILP) formulated as [38].

$$\min_{\boldsymbol{x}} f^T \boldsymbol{x} : \; A \cdot \boldsymbol{x} \leq b, \quad lb \leq x \leq ub$$

The vectors *lb*, *ub*, matrices *A* and corresponding vector $\boldsymbol{b}$ and a set of indices integer constraints (*intcon*) were initialized. Following initialization, the MILP solver is run to solve the problem for vector $\boldsymbol{x}$, where $f(x)$ is the coefficient matrix of the objective function, *lb* and *ub* are lower and upper bounds respectively. Since this is an assignment problem, x can only be binary, such that $lb = 0$, and $ub = 1$. The solver (*intlinprog*) involves the following main steps [38]:

- Reducing the problem size using linear program pre-processing.
- Solve an initial relaxed (non-integer) problem using linear programming (dual-simplex method). The objective functions and constraints remain the same, but any integer constraints are removed.
- Perform mixed-integer program pre-processing to tighten the linear programming relaxation of the mixed-integer problem.
- Try ''Cut Generationâ to further tighten the linear programming relaxation of the mixed integer problem.
- Try to find integer-feasible solutions using heuristics
- Use a Branch and Bound (BnB) algorithm to search systematically for the optimal solution. This solves linear programming relaxations with restricted ranges of possible values of the integer variables. It attempts to generate a sequence of updated bounds on the optimal objective function value.
- The bud nodes continue to generate further nodes as it analyzes and discards the ones that do not improve the value of the objective function until it reaches an incumbent solution such that the absolute gap tolerance is 10^{-5}.

B. OPTIMAL SENSING DURATION IN A FRAME

In the objective function of problem P1, τ_s only appears in $(T - \tau_s - \tau_r)/TM$, but it is intertwined with $\tau_{i,j}$ by the constraint in (C4), hence, direct decomposition cannot be achieved. In the expression of the probability of detection and the probability of false alarm in (2) and (3), both $P_{d,i,j}$ and $P_{f,i,j}$ increase monotonically with decreasing ε, but it is practically desirable to have a high probability of detection but low probability of false alarm. Hence, the objective function in problem P1 can only achieve its maximum when constraint (C1) is at equality, which can be satisfied when the probability of detection for each user on channel j $P_{d,i,j} = P_{d,j}^{th}$. The proof to verify this is similar to that provided in [10]. The value of $P_{d,j}^{th}$ that satisfies this constraint (based on the OR - fusion rule) can be determined from (5) as

$$P_{d,j}^{th} = 1 - \exp\left(\frac{\log_e(1-\beta)}{\sum_{i=1}^{N} x_{i,j}}\right), \quad \forall j \in \{1, \ldots, M\}, \tag{30}$$

where β is the constraint on the cooperative probability of detection $Q_{D,j}$. Therefore, (2) is equivalent to

$$\varepsilon_{i,j} = \sqrt{\frac{2\gamma_{i,j}+1}{\tau_{i,j} f_s}} Q^{-1}(P_d^{th}) + \gamma_{i,j} + 1, \tag{31}$$

and (3) can then be expressed in terms of P_d^{th} as

$$P_{f,i,j} = Q\left(\sqrt{(2\gamma_{i,j}+1)} Q^{-1}\left(P_{d,j}^{th}\right) + \gamma_{i,j}\sqrt{\tau_{i,j} f_s}\right). \tag{32}$$

Hence, the first constraint can be eliminated. Moreover, since $C_{0,j} \gg C_{1,j}$, and $(1-Q_{F,j}) \gg (1-Q_{D,j})$ in general, the value of the first expression in bracket on the RHS in (22) dominates the average throughput. Furthermore, due to the consideration for a network where the number of assigned channels to each SU are not necessarily equal, there is a dependence of K_i on the value of $\tau_{i,j}$ for each SU. Therefore, by substituting $\tau_{i,j} = \bar{\tau}_{i,j} := \frac{\tau_s}{K_i}$, $\forall i = \{1, \cdots, N\}$, and $P_{d,i,j} = P_{d,j}^{th}$, problem P1 can be approximated as

Problem P4: with fixed $\tau_{i,j}$ and $\varepsilon_{i,j}$, given $\chi_{i,j}$

$$\max_{\tau_s} \sum_{j=1}^{M} \bar{R}|_{(\tau_{i,j}=\bar{\tau}_{i,j})} = \max_{\tau_s} \frac{T_t}{TM} \times \sum_{j=1}^{M}\prod_{i=1}^{N}(1 - P_{f,i,j}(^{\tau_s}/_{K_i}, P_{d,j}^{th}))^{x_{i,j}} P(H_0) C_{0,j}, \tag{33}$$

$$\text{subject to: } e_s + \frac{T_t}{M} p_t \sum_{j=1}^{M} \left\{ \prod_{i=1}^{N} (1 - x_{i,j} P_{f,i,j}) P(H_0) \right\} \leq \bar{e}_h, \tag{C1}$$

$$0 \leq \tau_s \leq (T - \tau_r), \tag{C2}$$

where $e_s = (p_s \tau_s + p_r \tau_r)$ and $T_t = (T - \tau_r - \tau_s)$.

The Gaussian Q-function expression in (29) can also be written in terms of the complementary error function for ease of mathematical analysis as

$$P_{f,i,j} = \frac{1}{\sqrt{2}}\, erfc\left(\frac{\sqrt{2\gamma_{i,j}+1}\, Q^{-1}(P_{d,j}^{th}) + \gamma_{i,j}\sqrt{\frac{f_s \tau_s}{K_i}}}{2} \right) \tag{34}$$

Using the same approach as in Section IV-A, problem P4 can be re-written in terms of logarithmic function as

$$\max_{\tau_s} \log_e \bar{R}|_{(\tau_{i,j}=\bar{\tau}_{i,j})} = \max_{\tau_s} \left\{ \log_e \frac{T_t}{TM} P(H_0) C_0 + \sum_{j=1}^{M}\sum_{i=1}^{N} x_{i,j} \log_e \left(1 - P_{f,i,j}(^{\tau_s}/_{K_i}, P_{d,j}^{th})\right) \right\}, \tag{35}$$

$$\text{subject to: } E_s + \frac{T_t}{M} p_t \sum_{j=1}^{M} \left\{ \prod_{i=1}^{N} (1 - x_{i,j} P_{f,i,j}) P(H_0) \right\} \leq \bar{e}_h, \tag{C1}$$

$$0 \leq \tau_s \leq (T - \tau_r). \tag{C2}$$

Properties of Problem P4: In order to verify the convexity or otherwise of problem P4, there is a need to show that the objective function in (33) or (35) is concave in the range $0 \leq \tau_s \leq (T - \tau_r)$. To satisfy this, the function should be monotonically increasing for $0 \leq \tau_s \leq \tau_s^{opt}$, and monotonically decreasing for $\tau_s^{opt} \leq \tau_s \leq (T - \tau_r)$, such that $R(\tau_s^{opt})$ is the only maximal in the entire range. Therefore, the objective function must satisfy three conditions as follows

1) The first order derivative must be positive at $\tau_s = 0$, i.e., $R'(\tau_s)|_{(\tau_s=0)} > 0$
2) It must be negative at $\tau_s = T - \tau_r$, i.e., $R'(\tau_s)|_{(\tau_s=T-\tau_r)} < 0$
3) The second order derivative must be negative, i.e., $R''(\tau_s) < 0$

Proof: The first two conditions together imply that there must be a point in $0 \leq \tau_s \leq T - \tau_r$ that maximizes $R(\tau_s)$. The first and the third conditions together infer that $R(\tau_s)$ is strictly increasing in the range $0 < \tau_s < \tau_s^{opt}$, while the second and the third conditions together indicate that $R(\tau_s)$ is strictly decreasing in the range $\tau_s^{opt} < \tau_s < T - \tau_r$. Therefore, the three conditions together imply that $R(\tau_s)$ attains a global maximum within the range $0 \leq \tau_s \leq T - \tau_r$. The first order derivative of the objective function can be expressed as in (36), as shown at the top of the next page. For the expression in (36) to be positive, the second expression on the RHS must be less than the first expression. In which case, it is necessary to show that (37), as shown at the top of the next page is satisfied.

In (37), as τ_s approaches a value very close to zero (e.g., 10^{-6}), the first expression on the RHS can be approximated to $-\frac{1}{T-\tau_r}$. Generally, $exp(.) < 1$ (for $P_f \leq 0.1$) while, the complementary error function $erfc. \leq 1$. Therefore, $\sqrt{\frac{2\pi f_s \tau_s}{K_i}} \approx 2$ (for the value of f_s as selected in Table 1). Hence, the second expression on the RHS takes a value close to $f_s \gamma_{i,j}$, which is obviously much greater than the first expression, i.e., $f_s \gamma_{i,j} \gg \frac{1}{T-\tau_r}$. Therefore, $\frac{\partial}{\partial \tau_s} R(\tau_s)|_{(\tau_s \approx 0)} > 0$ in (36) and the first condition is satisfied.

However, at τ_s very close to $T - \tau_r$, the value of the first expression in the RHS of (36) tends to negative infinity $(-\infty)$, while the second expression approximates to $-\frac{f_s \gamma_{i,j}\sqrt{K_i}}{2\pi f_s (T-\tau_r)}$. It is obvious that $\frac{f_s \gamma_{i,j}\sqrt{K_i}}{2\pi f_s (T-\tau_r)} < \infty$, satisfying the second condition that is, $\frac{\partial}{\partial \tau_s} R(\tau_s)|_{(\tau_s \approx T-\tau_r)} < 0$.

The second order derivative of the objective function can be expressed as (38), as shown at the top of the next page. Following the same logic, it can easily be seen that the first expression on the RHS of the second order derivative (38), denoted as A is a positive value for all values of τ_s. The denominator (numerator) of the second expression denoted as B is negative (positive) for all values of τ_s (for the same reason as stated earlier), making the second expression negative. Both the numerator and denominator of the third expression designated as C are positive. The fourth expression denoted as D is negative since its denominator (numerator) is negative (positive). Therefore, putting A, B, C and D together, the second order derivative in (38) is a negative value for all values of τ_s, that is, $\frac{\partial^2 R(\tau_s)}{\partial \tau_s^2} < 0$, satisfying the third condition. Figures 3a, 3b and 3c are the plots of the expressions in (33), (36) and (38), illustrating the behavior of the objective function, the first order derivative, the second order derivative respectively. The characteristic of the plots shown also validates the analysis that the objective function is concave, making P4 strictly convex in the range $0 < \tau_s < (T - \tau_r)$.

Therefore, $R(\tau_s)$ satisfied the three conditions that the objective function is strictly (unimodal) concave with respect to τ_s in the range $0 \leq \tau_s \leq (T - \tau_r)$.

$$\frac{\partial}{\partial \tau_s} R(\tau_s) = \frac{1}{\tau_r - T + \tau_s} - \frac{1}{M} \sum_{j=1}^{M} \sum_{i=1}^{N} x_{i,j} \frac{f_s \gamma_{i,j} \exp\left(-\left(\vartheta + \frac{\gamma_{i,j}\sqrt{\frac{f_s \tau_s}{K_i}}}{2} \right)^2 \right)}{\left(erfc\left(\vartheta + \frac{\gamma_{i,j}\sqrt{\frac{f_s \tau_s}{K_i}}}{2} \right) - 2 \right) \sqrt{\frac{2\pi f_s \tau_s}{K_i}}} \tag{36}$$

$$\frac{1}{\tau_r - T + \tau_s} > \sum_{i=1}^{N} x_{i,j} \frac{f_s \gamma_{i,j} \exp\left(-\left(\vartheta + \frac{\gamma_{i,j}\sqrt{\frac{f_s \tau_s}{K_i}}}{2} \right)^2 \right)}{\left(erfc\left(\vartheta + \frac{\gamma_{i,j}\sqrt{\frac{f_s \tau_s}{K_i}}}{2} \right) - 2 \right) \sqrt{\frac{2\pi f_s \tau_s}{K_i}}} \tag{37}$$

$$\begin{aligned} \frac{\partial^2}{\partial \tau_s^2} R(\tau_s) = & \underbrace{-\frac{1}{(\tau_r - T + \tau_s)^2}}_{A} \\ & + \frac{1}{M} \sum_{j=1}^{M} \sum_{i=1}^{N} x_{i,j} \Bigg\{ \underbrace{\frac{\sqrt{2} {f_s}^2 \gamma_{i,j} \exp\left(-\left(\vartheta + \frac{\gamma_{i,j}\sqrt{\frac{f_s \tau_s}{K_i}}}{2} \right)^2 \right)}{8 K_i^2 \sqrt{\pi} \left(\frac{erfc\left(\vartheta + \frac{\gamma_{i,j}\sqrt{\frac{f_s \tau_s}{K_i}}}{2} \right)}{\sqrt{2}} - 1 \right) \frac{(f_s \tau_s)^{3/2}}{K_i}}}_{B} \\ & \underbrace{- \frac{f_s \gamma_{i,j}^2 \exp\left(-2\left(\vartheta + \frac{\gamma_{i,j}\sqrt{\frac{f_s \tau_s}{K_i}}}{2} \right)^2 \right)}{8 K_i \pi \tau_s \left(\frac{erfc\left(\vartheta + \frac{\gamma_{i,j}\sqrt{\frac{f_s \tau_s}{K_i}}}{2} \right)}{\sqrt{2}} - 1 \right)^2}}_{C} + \underbrace{\frac{\sqrt{2} f_s \gamma_{i,j}^2 \exp\left(-\left(\vartheta + \frac{\gamma_{i,j}\sqrt{\frac{f_s \tau_s}{K_i}}}{2} \right)^2 \right) \left(\vartheta + \frac{\gamma_{i,j}\sqrt{\frac{f_s \tau_s}{K_i}}}{2} \right)}{8 K_i \sqrt{\pi} \tau_s \left(\frac{erfc\left(\vartheta + \frac{\gamma_{i,j}\sqrt{\frac{f_s \tau_s}{K_i}}}{2} \right)}{\sqrt{2}} - 1 \right)}}_{D} \Bigg\}, \\ \vartheta = & \sqrt{2\gamma_{i,j} + 1} Q^{-1}(P_{d,j}^{th}). \end{aligned} \tag{38}$$

Having proved that the objective function in P4 is a unimodal function, which by extension can also show that the first part of the constraint in (C1) of P4 is equally concave, the optimization problem in P4 can easily be solved as a convex problem. In order to do this, the problem is analyzed under two scenarios as follows.

Case 1 (Optimal Solution With Unconstrained Energy): Under this scenario, the operation of the energy harvested SU is not limited by energy, and the SU can achieve maximum average throughput. Figure 4a shows the characteristic of the problem under energy unconstrained situation. In this case, the solution to the problem can be obtained merely through the sensing-throughput trade-off based on the objective function in (32) and the accompanied constraint in (C2). The problem is strictly unimodal and there exists an optimal solution $\tau_{s,o}^*$, which can be determined using Golden section search method for a fixed $\tau_{i,j}, j \in \{1, \cdots, K_i\}, \forall i$.

Case 2 (Optimal Solution With Energy Constrained): In this case, the operation of the energy harvested SU is subject to the energy causality constraint. Fig. 4b illustrates the characteristic of the problem under energy constrained scenarios with the feasibility regions shown shaded. From the figure, the parameter $e_{c,n}|(\tau_s = 0) = \prod_{i=1}^{N}(1 - 0.5)^{x_{i,j}} p_t T$, while $e_{c,n}|(\tau_s = T - \tau_t) = p_s(T - \tau_r) + p_r \tau_r$. The intersection of the energy consumption curve and the energy harvested (i.e. when constraint (C1) is at equality) shows the possible sensing time $(\tau_{s,e})$ that could maximize the objective function in problem P4 while satisfying the energy causality.

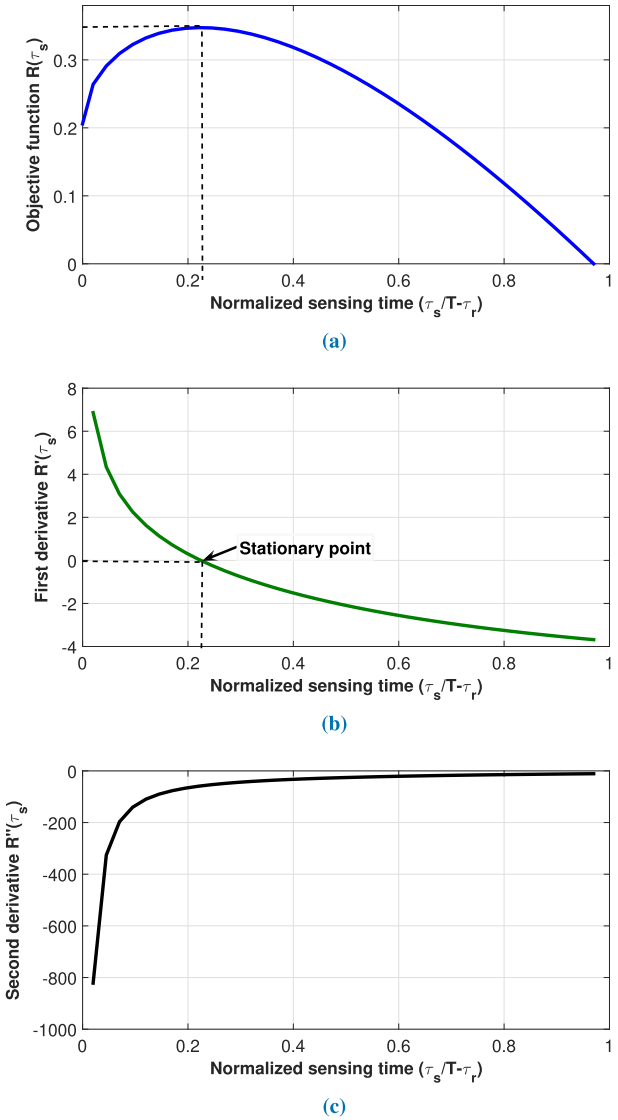

FIGURE 3. Plots of the objective function and the derivatives w.r.t. the normalized sensing time in problem P4 illustrating its concavity: (a) objective function, (b) the first order derivative, (c) second order derivative.

However, sensing time should be a small percentage of the total frame length (for sufficient data transmission time). Therefore, the optimal sensing duration can be obtained using Newton Raphson's method for a fixed $\tau_{i,j}, j \in \{1, \cdots, K_i\}, \forall i$ as

$$\tau^*_{s,e}: \ \min\left(f(\tau_{s,e}) = 0\right), \quad \textit{subject to: } 0 \le \tau_{s,e} \le (T - \tau_r), \tag{39}$$

where $f(\tau_{s,e})$ is (C1) in problem P4 when the constraint is at equality. Based on Newton-Raphson approach, the solution to (32) can be determined as

$$\tau^{k+1}_{s,e} = \tau^k_{s,e} \pm \frac{f(\tau^k_{s,e})}{f'(\tau^k_{s,e})}, \tag{40}$$

where the parameter k denotes an iteration index and $f'(\tau^k_{s,e})$ is the derivative of $f(\tau^k_{s,e})$, which is also formulated as constraint (C1) in problem P4. The general solution to problem P4 can therefore be expressed as $\tau_s^{opt} = \min(\tau^*_{s,o}, \tau^*_{s,e})$. Both $\tau^*_{s,o}$ and $\tau^*_{s,e}$ are as earlier defined under case 1 (the unconstrained energy region) and case 2 (constrained energy region) respectively.

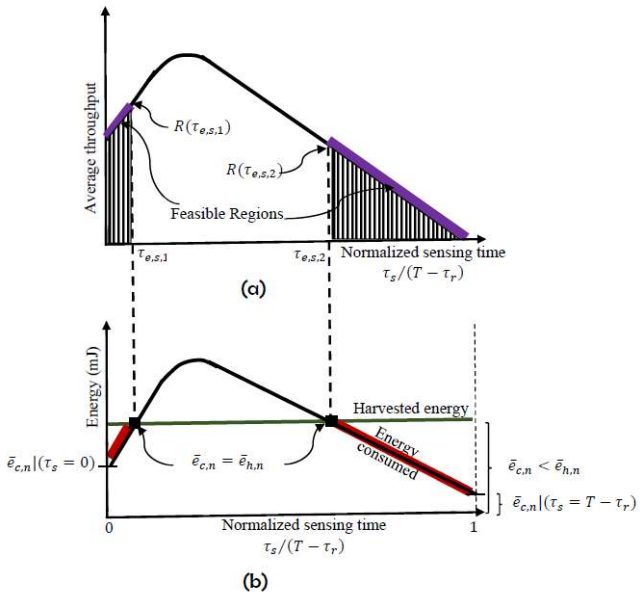

FIGURE 4. Characteristic curve of the problem P4 illustrating the feasibility regions for the energy constrained cognitive radio networks: (a) the objective function, (b) the energy constraint, where $e_{c,n}|(\tau_s = 0) = \prod_{i=1}^{N}(1 - 0.5)^{x_{i,j}} p_t T$, and $e_{c,n}|(\tau_s = T - \tau_t) = p_s(T - \tau_r) + p_r \tau_r$.

C. OPTIMAL SENSING PARAMETER PER CHANNEL

Given χ and τ_s, the optimal $\tau_{i,j}$ and $\varepsilon_{i,j}$ that maximize the objective function in problem P4 (with $\tau_{i,j}$ replacing τ_s/K_i) becomes

Problem P5:

$$\max_{\{\tau_{i,j}\},\{\varepsilon_{i,j}\}} \sum_{j=1}^{M} R(\tau_{i,j}, \varepsilon_{i,j})|_{(\tau_s=\tau_s^*, \chi=\chi^*)}$$

$$= \max_{\{\tau_{i,j}\},\{\varepsilon_{i,j}\}} \sum_{j=1}^{M} x_{i,j} \log_e(1 - P_{f,i,j}(\tau_{i,j}, P^{th}_{d,j}))P(H_0)C_{0,j}$$

$$\forall i \in \{1, \ldots, N\}, \tag{41}$$

$$\text{subject to: } \sum_{j=1}^{M} x_{i,j}\tau_{i,j} = \tau_s, \quad i \in \{1, \ldots, N\}, \tag{C1}$$

$$0 < \tau_{i,j} \le \tau_s, \quad i \in \{1, \ldots, N\}. \tag{C2}$$

However, since the problem in P5 is maximized with $P_{d,i,j} = P^{th}_{d,j}$, then the optimal detection threshold can be simply obtained, given $\tau^{opt}_{i,j}$, as

$$\varepsilon^{opt}_{i,j} = \sqrt{\frac{2\gamma_{i,j} + 1}{\tau^{opt}_{i,j} f_s}}\left(P^{th}_{d,j}\right) + \gamma_{i,j} + 1. \tag{42}$$

The problem then reduces to a single variable optimization as in

$$\sum_{j=1}^{M} x_{i,j} \frac{f_s \gamma_{i,j} \exp\left(-\left(\sqrt{(2\gamma_{i,j}+1)}\, Q^{-1}\left(P_{d,j}^{th}\right) + \frac{\gamma_{i,j}\sqrt{f_s \tau_{i,j}}}{2}\right)^2\right)}{\left(erfc\left(\sqrt{(2\gamma_{i,j}+1)}\, Q^{-1}\left(P_{d,j}^{th}\right) + \frac{\gamma_{i,j}\sqrt{f_s \tau_{i,j}}}{2}\right) - 2\right)\sqrt{2\pi f_s \tau_{i,j}}} - \lambda_j = 0 \tag{45}$$

$$\sum_{j=1}^{M} x_{i,j}\tau_{i,j} - \tau_s = 0, \quad \forall i \in \{1, \ldots, N\} \tag{46}$$

Problem P6:

$$\max_{\{\tau_{i,j}\}} \sum_{j=1}^{M} R(\tau_{i,j})|_{\tau_s=\tau_s^*} = \max_{\{\tau_{i,j}\}} \sum_{j=1}^{M} x_{i,j} \log_e(1 - P_{f,i,j}(\tau_{i,j}, P_d^{th}))P(H_0)C_{0,j} \quad \forall i \in \{1, \ldots, N\}, \tag{43}$$

$$\text{subject to: } \sum_{j=1}^{M} x_{i,j}\tau_{i,j} \le \tau_s, \quad i \in \{1, \ldots, N\}, \tag{C1}$$

$$0 < \tau_{i,j} \le \tau_s, \quad i \in \{1, \ldots, N\}. \tag{C2}$$

Following the approach used in Section IV-B, it can be easily verified that the objective function in problem P6 is a monotonically increasing concave function in the range $0 \le \tau_{i,j} \le \tau_s$ since the first and the third conditions are also satisfied in this case.

Using the Lagrangian multiplier approach, the Lagrangian $\mathcal{L}(\boldsymbol{\tau}, \boldsymbol{\lambda})$ of (39) is given by

$$\mathcal{L}(\boldsymbol{\tau}, \boldsymbol{\lambda}) = \sum_{j=1}^{M} x_{i,j} \log_e \left\{\left[1 - P_{f,i,j}(\tau_{i,j}, P_d^{th})\right] \times P(H_0)C_{0,j}\right\} - \lambda_j \left\{\sum_{j=1}^{M} x_{i,j}\tau_{i,j} - \tau_s\right\}, \quad \forall i \in \{1, \ldots, N\}$$
$$\text{subject to: } 0 < \tau_{i,j} \le \tau_s, \tag{44}$$

where $\boldsymbol{\tau} = \{\tau_{i,j}\}_{M \times N}$ is the channel sensing-time matrix, and $\boldsymbol{\lambda} = \{\lambda_j, \forall i = \{1, \cdots, N\}\}$ is the non-negative Lagrangian multiplier associated with the channel sensing-time distribution for each secondary user. The Lagrangian dual function is defined as $g(\boldsymbol{\lambda}) = \max_{\{\tau_{i,j}\}} \mathcal{L}(\boldsymbol{\tau}, \boldsymbol{\lambda})$, and the dual problem as $\min_{\boldsymbol{\lambda} \ge 0} g(\boldsymbol{\lambda})$. The Lagrange dual variable $\boldsymbol{\lambda}$ can be obtained by solving the corresponding optimization problem in P6 using the following Karush-Kuhn-Tucker (KKT) conditions in (45) and (46), as shown at the top of this page, whereby the derivative of the Lagrangian with respect to the optimal and the dual variables are each set to zero, and then obtain the optimal variable as a function of the dual. It is however, obvious that a closed form expression cannot be obtained for the dual variable, hence, the need to determine both the dual and primal variable iteratively using a sub-gradient approach. Both the primal and Lagrangian dual variables are iteratively updated as

$$\tau_{i,j}^{t+1} = \tau_{i,j}^{t} + \delta_{\boldsymbol{\tau}}, \quad i = 1, \cdots, N, \; j = 1, \cdots, M \tag{47}$$

$$\lambda_j^{t+1} = \lambda_j^{t} + \delta_{\boldsymbol{\lambda}}, \quad \forall i \in \{1, \cdots, N\} \tag{48}$$

until convergence towards a feasible optimal solution $\{\boldsymbol{\tau}^*, \boldsymbol{\lambda}^*\}$. The parameters $\delta_{\boldsymbol{\tau}}$ and $\delta_{\boldsymbol{\lambda}}$ denote step-sizes for the primal and the dual variables respectively. Algorithm 1 gives the summary of the solution method in Section IV

V. CONVERGENCE OF THE ALTERNATING CONVEX OPTIMIZATION

The analysis of the convergence and optimality of the procedure in Algorithm 1 is similar to that provided in [14], [39]. However, a brief explanation is given in this section. In the context of the alternating convex optimization, the following terms first need to be defined as given below [32].

Definition 1 (Marginally Optimum Coordinate): Let f be a function of two variables constrained to be in the sets X, Y respectively. For any point $y \in Y$, it can be said that $\hat{x}$ is a marginally optimal coordinate with respect to y, i.e., $\hat{x} \in mOPT_f(y)$, iff $(\hat{x}, y) \ge f(x, y)$ for all $x \in X$. Similarly for any $x \in X$, it can be said that $\hat{y} \in mOPT_f(x)$ if $\hat{y}$ is a marginally optimal coordinate with respect to x.

Definition 2 (Bistable Point): Given a function f over two variables constrained within the sets X, Y respectively, a point $(x, y) \in X \times Y$ is considered a bistable point if $y \in mOPT_f(x)$ and $x \in mOPT_f(y)$ i.e., both coordinates are marginally optimal with respect to each other.

Therefore, the optimum of the optimization problem must be a bistable point, and the procedure must converge after it has reached a bistable point. Although, the presented iterative algorithm may converge to a possible local maximum point, since the characteristic curve shown in Fig. 4 illustrates that the EH-CRN problem could have more than one bistable points, (one at τ_s close to zero, and the other at τ_s close to $(T - \tau_r)$). The bistable point to which the procedure converges depends on where the procedure is initialized between 0 and $(T - \tau_r)$.

However, taking into consideration that the sensing time must be a smaller fraction of the total frame length, the region of attraction for this problem is a bistable point selected as in (39). The objective function of the optimization problem in P1 is monotonically nondecreasing at every iteration, since it

Algorithm 1 Joint Channel Assignment and Cooperative Spectrum Sensing in Multichannel EH-CRN

procedure Channel Assignment and Sensing Parameter optimization.
Input β, K_{max}, n_{max}
  for $j = 1 : M$ **do**
    for $i = 1 : N$ **do**
Obtain the channel assignment $\chi = (x_{i,j})_{N\times M}$; giving τ_s and $\tau_{i,j}$ by solving problem P3 in section IV-A
- Generate the matrix $\Lambda = (p_{m,i,j})_{N\times M}$ at the CC based on the reported non-cooperative probability of miss-detection on all PUs from each SU. Here, $p_{m,i,j}$ (25) is the non-cooperative probability of miss-detection of PU j evaluated by SU i.
- Determine the channel assignment scheme / cluster formation following the method in [36].

$\chi^* \Leftarrow \chi$
Initialization $\delta \Leftarrow 0$
Repeat
Solve for optimal sensing duration $\boldsymbol{\tau}_s^*$ with fixed $\bar{\tau}_{i,j} := {}^{\tau_s^*}/_{K_i}$, giving χ^* in problem P4, section IV-B
- Obtain $\tau_{s,o}$ from the objective function in P4 based on a Golden Section search method (for unconstrained energy case).
- Determine $\tau_{s,e}$ from constraint C1 of problem P4 using Newton-Raphson method (for constrained energy case).
- $\tau_s^* \Leftarrow \min\{\tau_{s,o}, \tau_{s,e}\}$
- $\tau_s^{(\delta+1)} \Leftarrow \tau_s^*$

Solve for the optimal sensing time $\boldsymbol{\tau}_{i,j}^*$ for every SU i on channel j in problem P5 or P6, section IV-C: giving $\chi_{i,j}^*$ and τ_s^δ:
- Determine $\tau_{i,j}^*$ from problem P6 using Lagrangian multiplier method.
- $\tau_{i,j}^{(\delta+1)} \Leftarrow \tau_{i,j}^*$

$\delta \Leftarrow (\delta + 1)$
until $\tau_s^\delta == \tau_s^{\delta-1}$, $\tau_{i,j}^\delta == \tau_{i,j}^{\delta-1}$
Determine the detection threshold $\boldsymbol{\varepsilon}_{i,j}^*$ from (42)
    end for
  end for
Output: χ^*, τ_s^*, $\{\tau_{i,j}^*\}$, $\{\varepsilon_{i,j}^*\}$,
end procedure

can be concluded from Algorithm 1 that

$$R(\tau_s^\delta, \tau_{i,j}^\delta, \varepsilon_{i,j}^\delta) \leq R\left(\tau_s^{(\delta+1)}, \tau_{i,j}^\delta, \varepsilon_{i,j}^\delta\right) \leq R\left(\tau_s^{(\delta+1)}, \tau_{i,j}^{(\delta+1)}, \varepsilon_{i,j}^{(\delta+1)}\right), \quad \forall\delta. \tag{49}$$

Notwithstanding, the expression is upper bounded in the extreme scenario with $\tau_s^* = 0$, and $Q_{f,j} = 0$ as $\mathbb{E}\left\{\frac{T-\tau_r}{TM}\sum_{j=1}^{M}\left(P(H_0)C_{0,j} + (1-\beta)P(H_1)C_{1,j}\right)\right\}$, which indicates that it converges [21], [39]. In this particular case, the value of the objective function remains unchanged after a single iteration. Nevertheless, since the original problem is jointly non-convex in the optimization variables and the problem structure could have more than one bistable point, the convergence could only be guarantee to reach a local optimum.

VI. SIMULATION RESULTS

This section presents the simulation results of the energy harvesting cognitive radio network. The channel assignment is centrally implemented at the secondary user Base Station (SBS) based on outdated CSI, while the spectrum sensing and opportunistic energy harvesting are distributed. The network consists of varying number of PU channels and SUs randomly deployed in a $5km \times 5km$ square area. This becomes necessary in order to evaluate the performance of the multichannel CRN under varying number of assigned PU channels to each SU. The average number of assigned channels to each SU is dependent on the ratio of SUs to PU channels in the network [36]. For the simulations, the system parameters are summarized in Table 1, which are drawn mainly from [6]. In addition, the following parameter values are used: $L = 50$, $u = 5$, $\mu = 3$, $\kappa = 1.0$ [40] and [41]. The parameters $\epsilon_{i,j}$ and $F_{i,j}^{max}$ are chosen randomly as $0.001sec \leq \epsilon_{i,j} \leq 10sec$, and $1 \leq F_{d,i,j}^{max} \leq 7$ respectively in order to obtain different correlation factor $\rho_{i,j}$. The primary user's transmit power P_{PU} and the noise power N_0 are chosen as $50mW$ and $-90dBm$ respectively ([40] and [41]), in agreement with standard values, while the average SNR of PU j at SU i terminal ($\bar{\gamma}_{i,j}$) is evaluated based on the inverse square law.

TABLE 1. System parameters.

Symbol	Description	Value
u	Time-bandwidth product	5
f_s	Sampling frequency	1 MHz
p_s	Sensing power	110 mW
p_t	Transmission power	410 mW
p_r	Reporting power	410 mW
T	Frame duration	200 ms
τ_r	Reporting time	50 ms
P_{PU}	Primary user transmit power	1 W
$\bar{\xi}^s$	Mean SNR value of SU on the transmit channel	20 dB [12]
$\bar{\xi}^p$	Mean SNR value of PU on the transmit channel	-15 dB [12]
$P(H_0)$	Probability that channel is not occupied by PU	0.8 dB
$P(H_1)$	Probability that a channel is occupied by PU	0.2 dB
N_0	Noise power	-90 dBm
β	Target probability of detection	0.9

A. PERFORMANCE OF CRN WITH SINGLE RF HARVESTING SOURCE

Under this scenario, the values of N and M are set to 20 and 15 respectively. Therefore, based on this ratio, different number of PU channels are assigned to each SU across the network. Each SU is required to sense the assigned channels within the same sensing period τ_s^{opt}. However, the SU can only harvest RF energy from one source, which might be a dedicated RF source or its elect transmit channel. Results show that optimal sensing period in a frame increases with

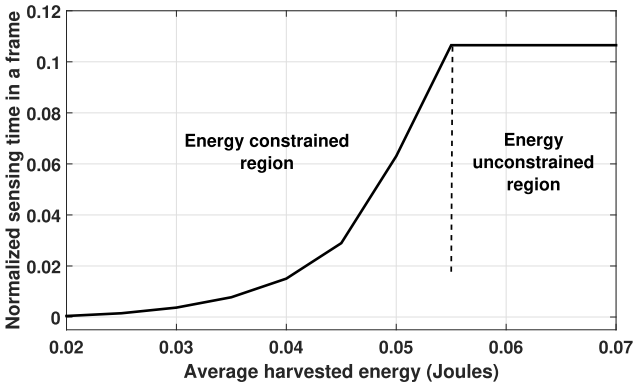

FIGURE 5. Plot showing the variation of sensing duration in a frame τ_s^{opt} with the harvested energy in the secondary user: $N = 25$, $M = 15$.

the amount of harvested energy in the energy constrained region as shown in Fig. 5. The behavior of the plot in Fig.5 is similar to that obtained by Chung *et al* in [8] for a single SU, single channel case. The results In Figs. 6a and 6b show the optimal sensing time that maximizes average throughput and the average throughput to consumption ratio with increasing sensing duration (harvested energy). Interestingly, these results illustrate that there exists different optimal sensing duration that maximizes these two metrics. Average throughput to consumption ratio is seen to be maximized at a smaller sensing time.

Fig. 7 shows the sensing time distribution among the channels assigned to each SU in an overlapping cluster scheme. The figure only shows the first ten secondary users in the network for clarity. The sensing time on each channel is directly related to the magnitude of the received SNR of the PUs at the terminals of the SU. Hence, the sensing time are distributed such that its optimal pairing with the detection threshold and SNR of each PU signal at the SUs' terminal can achieve the target probability of detection on each channel (or cluster). As a result, channel with low SNR requires a larger sensing time than the one with smaller SNR in order to achieve the same sensing accuracy.

B. PERFORMANCE OF CRN WITH MULTIPLE RF HARVESTING SOURCES

The performance of the CRNs with multiple PU harvesting sources is hereby analyzed. Each SU is required to sense the assigned channels and opportunistically harvest RF energy from any of the assigned channels. Simulation result shows that the amount of energy harvested increases with the RF harvesting sources, and sensing time in a frame is equally enhanced with increasing number of channel (or PU harvesting sources) assigned per SU as shown in Fig. 8. Very importantly, Fig. 9 shows that average harvesting to consumption energy ratio (otherwise refers to as active probability) can increase with increasing number of assigned PU harvesting sources. The result in Fig. 10a presents the relationship between the average achievable throughput and

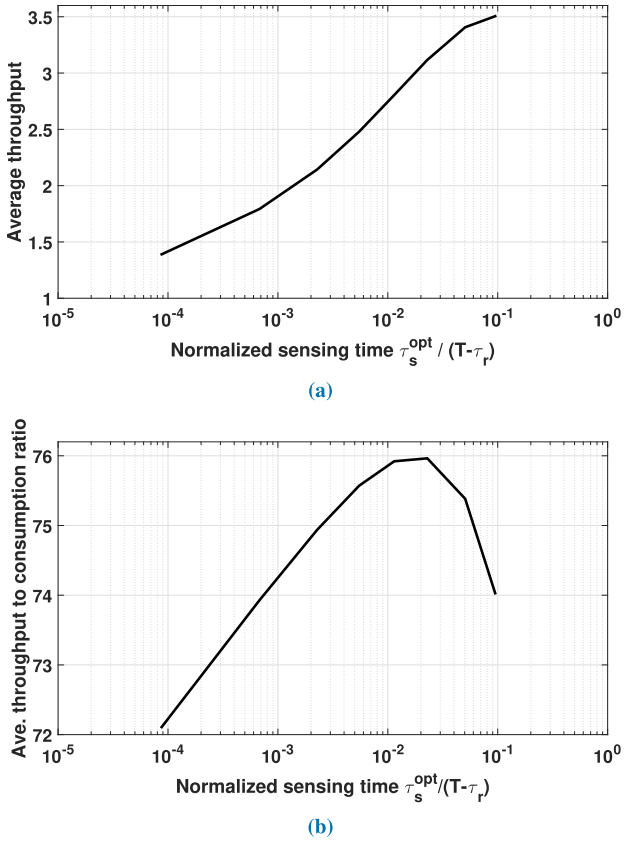

FIGURE 6. Optimal sensing duration $\tau_s^{opt}/(T-\tau_r)$ for throughput and energy efficiency: (a) average throughput (b) average throughput to consumption ratio $N = 25$, $M = 15$.

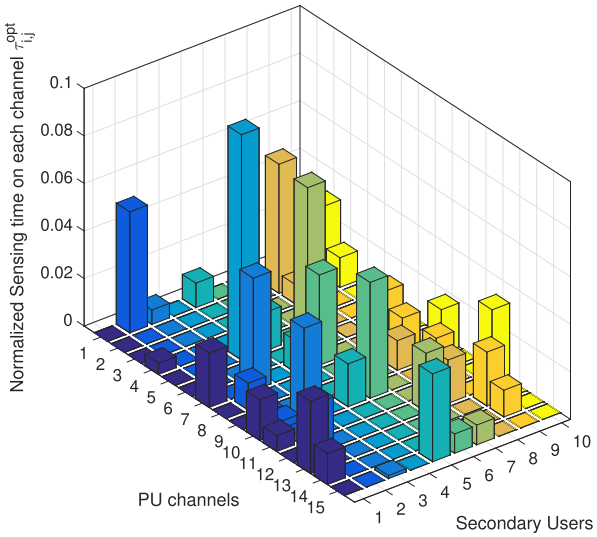

FIGURE 7. Optimal sensing time of each secondary user on the assigned PU channels $\tau_{i,j}^{opt}$: $N = 25$, $M = 15$.

the number of RF harvesting sources. It shows that there is initial increase in the achievable throughput with increasing number of harvesting sources, which is reversed after a particular threshold. The logical explanation for this is that,

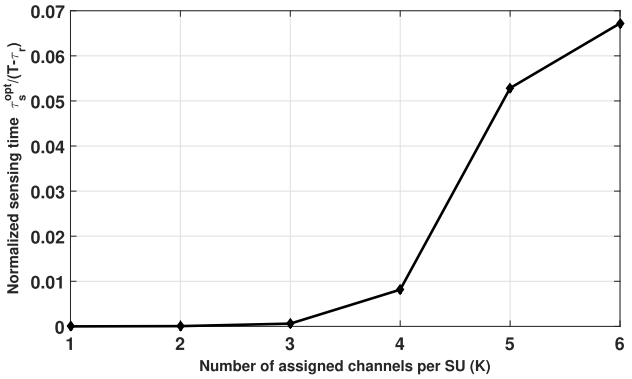

FIGURE 8. Optimal sensing duration corresponding to the number of RF harvesting sources K_i. Note that the SU can harvest RF from only one busy channel in a frame: $N = 30$, $M = 25$, $P_{avail} = 0.5Watts$.

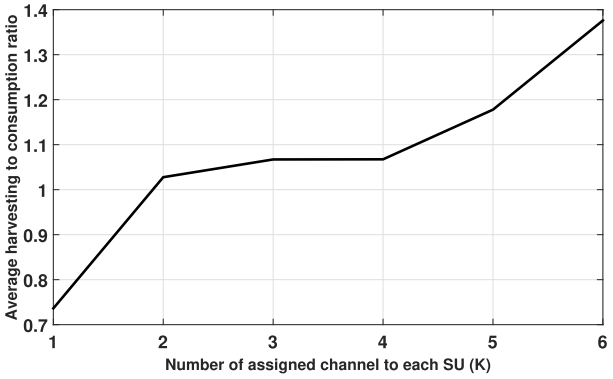

FIGURE 9. Active probability corresponding to the number of RF harvesting sources K_i: $N = 30$, $M = 25$, $P_{avail} = 0.5Watts$.

increasing the number of RF harvesting sources enhances the energy budget and allows for adequate sensing period for better sensing accuracy. As sensing accuracy improves in terms of reduced false alarm rate, average throughput increases.

On the other hand, as the number of assigned RF harvesting sources increases, more channels are sensed, leading to increase in sensing time. As a result, the data transmission time reduces resulting in reduced average throughput. Therefore, a trade off exists between the number of RF sources (available for spectrum sensing and opportunistic energy harvesting), and the average throughput, and an optimal number of RF sources therefore exist, which maximizes the average throughput. In the same vein in Fig. 10b, the amount of energy consumption increases with the number of RF harvesting sources, since this brings about an increase in both sensing energy due to increased sensing time and data transmission energy (courtesy of improved sensing accuracy). The figure shows that energy consumption is largest when throughput is at its peak. On the other hand, as more channels are sensed, increasing the sensing time, there is a continuous increase in sensing energy but a decline in data transmission energy due to the reduced data transmission time. The overall effect is a reduction of energy consumption since the effect of

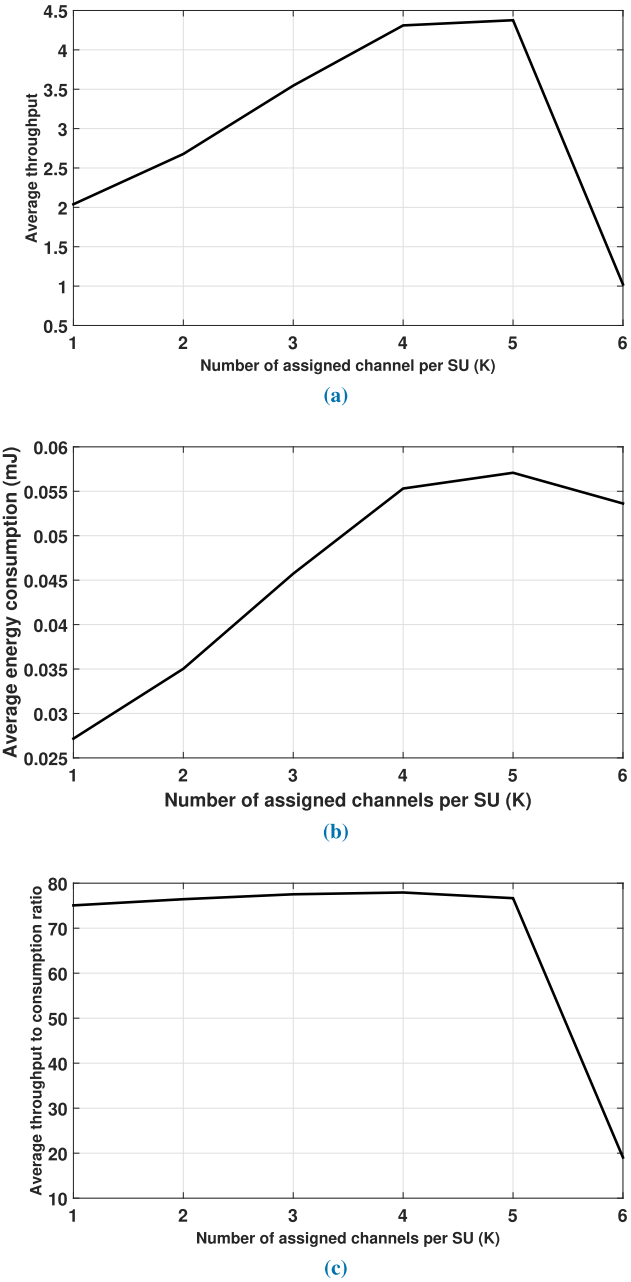

FIGURE 10. Performance of the energy harvesting cognitive radio networks with multiple RF harvesting sources K_i: (a) average throughput (b) average consumption and (c) average throughput to consumption ratio: $N = 30$, $M = 25$, $P_{avail} = 0.5Watts$.

the loss of transmission energy is greater that the effect of the gain in sensing energy. This accounts for the gradual decline in energy consumption as shown in Fig. 10b.

Fig. 10c illustrates the relationship between average throughput to consumption ratio, (which can otherwise be referred to as energy efficiency) and the number of assigned PU channels. This result shows that maximum numbers of RF harvesting sources exist over which the energy efficiency can be maximized. Within this region, both throughput and consumption increase at almost equal proportion with

increasing number of RF harvesting sources. However, it can be observed that throughput to consumption ratio is maximized at a lower number of RF sources than the average throughput and consumption. While both average throughput and consumption peak at $K = 5$, the ratio of average throughput to consumption is maximum at $K = 4$. Nevertheless there is a rapid decline in the average throughput and throughput to consumption ratio at $K = 5$.

Comparing with the work presented in e.g. [8], the results shown in Figs. 8, 9 and 10a provide insights into how to practically achieve better performance in the EH-CRNs. These results illustrate the performance gains that could be achieved, and the losses that could be incurred in EH-CRNs in terms of sensing time, the active probability of SUs and the achievable throughput with increasing number of radio frequency harvesting sources.

VII. CONCLUSION

The work presented in this paper has investigated an optimal multichannel cooperative spectrum sensing in an energy harvesting based cognitive radio networks. This involves determining the total sensing time needed by any secondary user in a frame and how to distribute the total sensing time among all the assigned channels in cooperative hard decision spectrum sensing. The initial non-convex, mixed integer nonlinear problem is transformed into a multiple convex optimization problem, which is then solved using alternating convex optimization technique. Simulation results obtained show that the considered work can improve the active probability of the SUs by exploiting the multi-channel benefit of practical CRN. Nevertheless, an optimum number of PU energy harvesting sources exits which maximizes the average achievable throughput and average throughput to consumption ratio in the energy harvesting based multi-channel cognitive radio networks.

REFERENCES

[1] J. A. Paradiso and T. Starner, "Energy scavenging for mobile and wireless electronics," *IEEE Pervasive Comput.*, vol. 4, no. 1, pp. 18–27, Jan./Mar. 2005. doi: 10.1109/MPRV.2005.9.

[2] A. Harb, "Energy harvesting: State-of-the-art," *Renew. Energy*, vol. 36, no. 10, pp. 2641–2654, 2011.

[3] I. Krikidis, S. Timotheou, S. Nikolaou, G. Zheng, D. W. K. Ng, and R. Schober, "Simultaneous wireless information and power transfer in modern communication systems," *IEEE Commun. Mag.*, vol. 52, no. 11, pp. 104–110, Nov. 2014. doi: 10.1109/MCOM.2014.6957150.

[4] M.-L. Ku, W. Li, Y. Chen, and K. J. R. Liu, "Advances in energy harvesting communications: Past, present, and future challenges," *IEEE Commun. Surveys Tuts.*, vol. 18, no. 2, pp. 1384–1412, 2nd Quart. 2016. doi: 10.1109/COMST.2015.2497324.

[5] Y.-C. Liang, Y. Zeng, E. C. Y. Peh, and A. T. Hoang, "Sensing-throughput tradeoff for cognitive radio networks," *IEEE Trans. Wireless Commun.*, vol. 7, no. 4, pp. 1326–1337, Apr. 2008. doi: 10.1109/TWC.2008.060869.

[6] S. Park, H. Kim, and D. Hong, "Cognitive radio networks with energy harvesting," *IEEE Trans. Wireless Commun.*, vol. 12, no. 3, pp. 1386–1397, Mar. 2013. doi: 10.1109/TWC.2013.012413.121009.

[7] S. Park and D. Hong, "Optimal spectrum access for energy harvesting cognitive radio networks," *IEEE Trans. Wireless Commun.*, vol. 12, no. 12, pp. 6166–6179, Dec. 2013. doi: 10.1109/TWC.2013.103113.130018.

[8] W. Chung, S. Park, S. Lim, and D. Hong, "Spectrum sensing optimization for energy-harvesting cognitive radio systems," *IEEE Trans. Wireless Commun.*, vol. 13, no. 5, pp. 2601–2613, May 2014. doi: 10.1109/TWC.2014.032514.130637.

[9] S. Park and D. Hong, "Achievable throughput of energy harvesting cognitive radio networks," *IEEE Trans. Wireless Commun.*, vol. 13, no. 2, pp. 1010–1022, Feb. 2014. doi: 10.1109/TWC.2013.121713.130820.

[10] Y. C. Liang, Y. Zeng, E. C. Y. Peh, and A. T. Hoang, "Sensing-throughput tradeoff for cognitive radio networks," *IEEE Trans. Wireless Commun.*, vol. 7, no. 4, pp. 1326–1337, Apr. 2008.

[11] S. Yin, Z. Qu, and S. Li, "Achievable throughput optimization in energy harvesting cognitive radio systems," *IEEE J. Sel. Areas Commun.*, vol. 33, no. 3, pp. 407–422, Mar. 2015. doi: 10.1109/JSAC.2015.2391712.

[12] G. Han, J.-K. Zhang, and X. Mu, "Joint optimization of energy harvesting and detection threshold for energy harvesting cognitive radio networks," *IEEE Access*, vol. 4, pp. 7212–7222, 2016.

[13] S. K. Nobar, K. A. Mehr, and J. M. Niya, "RF-powered green cognitive radio networks: Architecture and performance analysis," *IEEE Commun. Lett.*, vol. 21, no. 2, pp. 296–299, Feb. 2016.

[14] S. Biswas, A. Shirazinia, and S. Dey, "Sensing throughput optimization in cognitive fading multiple access channels with energy harvesting secondary transmitters," in *Proc. 24th Eur. Signal Process. Conf. (EUSIPCO)*, Aug. 2016, pp. 577–581. doi: 10.1109/EUSIPCO.2016.7760314.

[15] A. Celik, A. Alsharoa, and A. El Kamal, "Hybrid energy harvesting-based cooperative spectrum sensing and access in heterogeneous cognitive radio networks," *IEEE Trans. Cogn. Commun. Netw.*, vol. 3, no. 1, pp. 37–48, Mar. 2017. doi: 10.1109/TCCN.2017.2653185.

[16] Pratibha and K. H. Li and K. C. Teh, "Dynamic cooperative sensing–access policy for energy-harvesting cognitive radio systems," *IEEE Trans. Veh. Technol.*, vol. 65, no. 12, pp. 10137–10141, Dec. 2016.

[17] A. Bhowmick, S. D. Roy, and S. Kundu, "Throughput of a cognitive radio network with energy-harvesting based on primary user signal," *IEEE Wireless Commun. Lett.*, vol. 5, no. 2, pp. 136–139, Apr. 2016.

[18] A. Banerjee, S. P. Maity, and R. K. Das, "On throughput maximization in cooperative cognitive radio networks with eavesdropping," *IEEE Commun. Lett.*, vol. 23, no. 1, pp. 120–123, Jan. 2019.

[19] A. Banerjee and S. P. Maity, "On residual energy maximization in cognitive relay networks with eavesdropping," *IEEE Syst. J.*, to be published.

[20] A. Bhowmick, K. Yadav, and S. D. Roy, "Throughput of an energy harvesting cognitive radio network based on prediction of primary user," *IEEE Trans. Veh. Technol.*, vol. 66, no. 9, pp. 8119–8128, Sep. 2017.

[21] X. Liu, F. Li, and Z. Na, "Optimal resource allocation in simultaneous cooperative spectrum sensing and energy harvesting for multichannel cognitive radio," *IEEE Access*, vol. 5, pp. 3801–3812, 2017.

[22] Y. Gao, H. He, Z. Deng, and X. Zhang, "Cognitive radio network with energy-harvesting based on primary and secondary user signals," *IEEE Access*, vol. 6, pp. 9081–9090, 2018.

[23] Y. Yao, C. Yin, X. Song, and N. C. Beaulieu, "Increasing throughput in energy-based opportunistic spectrum access energy harvesting cognitive radio networks," *J. Commun. Netw.*, vol. 18, no. 3, pp. 340–350, Jun. 2016.

[24] A. Alsharoa, N. M. Neihart, S. W. Kim, and A. El Kamal, "Multi-band RF energy and spectrum harvesting in cognitive radio networks," in *Proc. IEEE Int. Conf. Commun. (ICC)*, May 2018, pp. 1–6.

[25] M. Xu, M. Jin, Q. Guo, and Y. Li, "Multichannel selection for cognitive radio networks with RF energy harvesting," *IEEE Wireless Commun. Lett.*, vol. 7, no. 2, pp. 178–181, Apr. 2018.

[26] R. Fan and H. Jiang, "Optimal multi-channel cooperative sensing in cognitive radio networks," *IEEE Trans. Wireless Commun.*, vol. 9, no. 3, pp. 1128–1138, Mar. 2010. doi: 10.1109/TWC.2010.03.090467.

[27] M. L. Puterman, *Markov Decision Processes: Discrete Stochastic Dynamic Programming*, 1st ed. Hoboken, NJ, USA: Wiley, 2005.

[28] S. H. A. Ahmad, M. Liu, T. Javidi, Q. Zhao, and B. Krishnamachari, "Optimality of myopic sensing in multichannel opportunistic access," *IEEE Trans. Inf. Theory*, vol. 55, no. 9, pp. 4040–4050, Sep. 2009.

[29] K. Wang, L. Chen, K. A. Agha, and Q. Liu, "On optimality of myopic policy in opportunistic spectrum access: The case of sensing multiple channels and accessing one channel," *IEEE Wireless Commun. Lett.*, vol. 1, no. 5, pp. 452–455, Oct. 2012.

[30] K. Wang, L. Chen, and Q. Liu, "On optimality of myopic policy for opportunistic access with nonidentical channels and imperfect sensing," *IEEE Trans. Veh. Technol.*, vol. 63, no. 5, pp. 2478–2483, Jun. 2014.

[31] A. Beck, "On the convergence of alternating minimization with applications to iteratively reweighted least squares and decomposition schemes," *SIAM J. Optim.*, vol. 25, no. 1, pp. 185–209, 2015.

[32] P. Jain and P. Kar, "Non-convex optimization for machine learning," *Found. Trends Mach. Learn.*, vol. 10, nos. 3–4, pp. 142–336, 2017. doi: 10.1561/2200000058.
[33] A. A. Alkheir and H. T. Mouftah, "An improved energy detector using outdated channel state information," *IEEE Commun. Lett.*, vol. 19, no. 7, pp. 1237–1240, Jul. 2015.
[34] G. M. Dillard, "Recursive computation of the generalized Q function," *IEEE Trans. Aerosp. Electron. Syst.*, vol. AES-9, no. 4, pp. 614–615, Jul. 1973.
[35] W. Zhang, R. K. Mallik, and K. B. Letaief, "Optimization of cooperative spectrum sensing with energy detection in cognitive radio networks," *IEEE Trans. Wireless Commun.*, vol. 8, no. 12, pp. 5761–5766, Dec. 2009.
[36] A. A. Olawole, F. Takawira, and O. O. Oyerinde, "Channel assignment scheme in clustered multi-channel cognitive radio networks with outdated CSI over Rayleigh fading channels," *Int. J. Commun. Syst.*, vol. 31, no. 14, Jul. 2018.
[37] A. Bander and E. Waleed, "Resource management for cognitive IoT systems with RF energy harvesting in smart cities," *IEEE Access*, to be published. doi: 10.1109/ACCESS.2018.2874134.
[38] *MATLAB—Optimization Toolbox Users' Guide*, The MathWorks, Natick, MA, USA, 2018.
[39] E. C. Y. Peh, Y.-C. Liang, Y. L. Guan, and Y. Zeng, "Optimization of cooperative sensing in cognitive radio networks: A sensing-throughput tradeoff view," *IEEE Trans. Veh. Technol.*, vol. 58, no. 9, pp. 5294–5299, Nov. 2009.
[40] W. Wang, B. Kasiri, J. Cai, and A. S. Alfa, "Channel assignment schemes for cooperative spectrum sensing in multi-channel cognitive radio networks," *Wireless Commun. Mobile Comput.*, vol. 15, no. 10, pp. 1471–1484, 2013.
[41] W. Saad, Z. Han, T. Basar, M. Debbah, and A. Hjørungnes, "Coalition formation games for collaborative spectrum sensing," *IEEE Trans. Veh. Technol.*, vol. 60, no. 1, pp. 276–297, Jan. 2011.

AKINBODE A. OLAWOLE received the B.Sc. (Hons.) and M.Sc. degrees in electronic and electrical engineering from Obafemi Awolowo University, Ile-Ife, Nigeria, and the Ph.D. degree in electrical engineering from the School of Electrical and Information Engineering, University of the Witwatersrand, Johannesburg, South Africa. He has held appointment with the Nigerian Television Authority (NTA), Nigeria, and has been a Member of Academic Staff of Obafemi Awolowo University, since 2007 till date though currently on leave in pursuance of his Ph.D. with the University of the Witwatersrand. His area of current research includes cognitive radio networks and resource management for wireless and mobile networks.

FAMBIRAI TAKAWIRA received the B.Sc. degree (Hons.) in electrical and electronic engineering from The University of Manchester, Manchester, U.K., in 1981, and the Ph.D. degree from Cambridge University, Cambridge, U.K., in 1984. After 19 years at the University of KwaZulu-Natal (UKZN), Durban, South Africa, in 2012, he joined the University of the Witwatersrand at Johannesburg, Johannesburg, South Africa. At UKZN, he held various academic positions, including that of the Head of the School of Electrical, Electronic, and Computer Engineering and, just before his departure, the Dean of the Faculty of Engineering. He has also held appointments at the University of Zimbabwe, Harare, Zimbabwe; the University of California at San Diego, San Diego, CA, USA; British Telecom Research Laboratories; and the National University of Singapore, Singapore. His research interests include wireless communication systems and networks. He is a Past Editor of the IEEE TRANSACTIONS ON WIRELESS COMMUNICATIONS. He has served on several conferences organizing committees. He served as the Communications Society Director of the Europe, Middle East, and Africa region, from 2012 to 2013.

OLUTAYO O. OYERINDE received the Ph.D. degree in electronic engineering from the University of Kwazulu-Natal, Durban, South Africa, in 2011. He has been with the School of Electrical and Information Engineering, University of the Witwatersrand at Johannesburg, South Africa, since 2013, where he is currently a Senior Lecturer. His current research interests include wireless communications with specific interests in 5G and beyond 5G technologies, including OFDM systems, NOMA systems, massive MIMO, mmWave massive MIMO, channels estimation, multiuser detection, and other signal processing techniques for wireless communication systems. He is an National Research Foundation (NRF) rated scientist, a Registered Professional Engineer (Pr.Eng.) with the Engineering Council of South Africa (ECSA), a Registered Engineer (R.Eng) with COREN, a Senior Member of Institute of Electrical and Electronics Engineer (SMIEEE), and a Corporate Member of NSE amongst others. He is an Editorial Board Member of the *International Journal of Sensors, Wireless Communications and Control*.